Experimental Study on the Damage Evolution of Rebar-Concrete Interface

Lu Xinzheng

SCHOOL OF CIVIL AND STRUCTURAL ENGINEERING

NANYANG TECHNOLOGICAL UNIVERSITY

1999/2000

ABSTRACT

In reinforced concrete structures, the bonding between concrete and steel bar is one of the most important factors that enable these two different materials to work together. In order to derive a better understanding of the bond properties and to apply it to the damage model of concrete, a new type of bond-slip test has been developed in this study. From the test results, the constitutive relationship of bond-slip is obtained and then used in the finite element analysis. The computation results are found to be consistent with the test results. Hence, this constitutive relationship can be applied in the numerical analysis. Besides, the distribution of the slip field and bond stress field is also obtained from the numerical computation. The slip field satisfied the assumption made in Liu Yu's constitutive model, which is based on the damage mechanics.

ACKNOWLEDGEMENT

Fist I would like to express my deep gratitude to my supervisor, A/P Soh Chee Kiong, for his support and encouragement throughout the project.

I would also like to express my sincere appreciation to Dr. Dong Yuexing and RS. Liu Yu. They gave me guidance and direction throughout the period of study. RS. Liu also did the whole test with me together. Without their help, I can't finish my work in so short time.

Prof. Jiang Jianjing, who is my supervisor in Tinghua University, cared for my work all along and wrote to me many times to give me advise and encouragement. I express my sincere appreciation for his kindness.

When I process my test, technicians in Construction Lab, Heavy Structure Lab and Structure Mechanics Lab all give me great help. I also express my appreciation to them.

Finally, I express my appreciation to the Tan Chin Tuan Exchange Student Scholarship Foundation. Thanks for they provide the study chance in NTU to me.

This report consists of three main parts. The first part (Chapter 2) introduces the device and the procedure of the experiment. The second part (Chapter 3) is the test data analysis. An empirical bond-slip relationship formula is proposed based on the experimental curves. The third part (Chapter 4) introduces the numerical computation and compares the computation result to the test result and good agreement is achieved.

CONTENT

LIST OF FIGURES

LIST OF TABLES

NOTATIONS

D_s	Bonding-slip local damage
Δ_1	Relative slip between concrete and rebar on top surface
Δ_2	Relative slip between concrete and rebar on bottom surface
δ_1	Deformation of concrete on top surface
δ_2	Deformation of concrete on bottom surface
h	Height of specimen
F	Axial force of the steel bar
D	Diameter of the steel bar
Δu	Difference of the steel bar displacement between the top and the bottom surface.
$\bar{\tau}$	Average bonding stress
τ_1	Maximum bonding stress
τ_2	Minimum bonding stress

Chapter 1 Introduction

Concrete is one of the most widely used construction materials. With the development of science and technology, many new types of concrete buildings are built in which concrete is often under complex stress conditions. In order to explain the behavior of concrete under such conditions, the constitutive relationship of concrete should be carefully studied. In recent years, the damage model for concrete is developing very fast, with many new constitutive models emerged in the literature. Since 1999, a new damage model based on geometrical consideration has been developed by Liu Yu, referring to Liu's First Year Report (reference [1]). In his model, concrete is treated as a homogeneous material. The damage in concrete due to loading is assumed to be penny-shaped micro-cracks or meso-cracks. And the flaw in concrete before load is not taken into account. In order to depict the defects in concrete a second order damage tensor D is used.

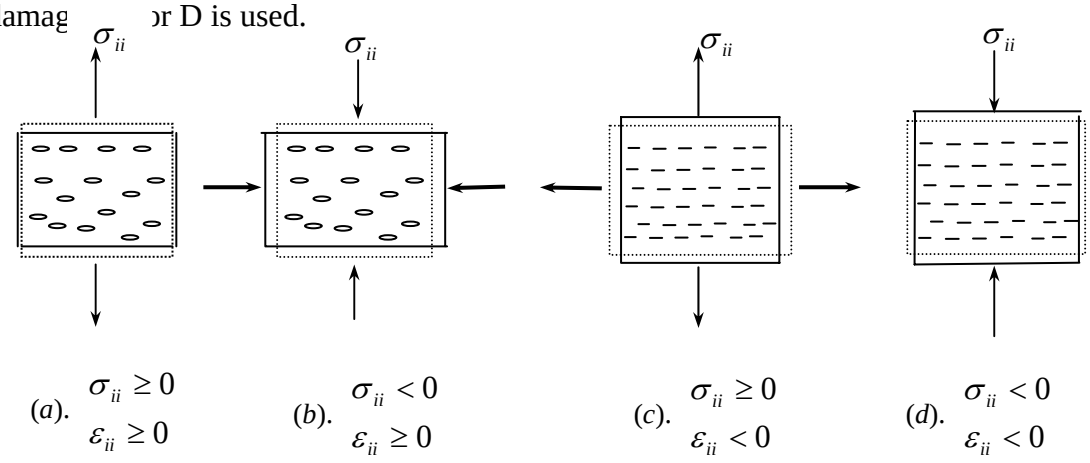

Figure 1.1 Definition of effective damage tensor

In Liu's model, for the principal damage coordinate system, the effective principal damage components are defined as

$$\tilde{D}_i = \begin{cases} D_i & when \ \sigma_{ii} \geq 0 \quad or \quad \varepsilon_{ii} \geq 0 \\ 0 & \sigma_{ii} < 0 \ and \quad \varepsilon_{ii} < 0 \end{cases} \tag{1-1}$$

So, the damage tensor in the principal damage coordinate system is

$$\tilde{D} = \begin{Bmatrix} \tilde{D}_1 \\ \tilde{D}_2 \\ \tilde{D}_3 \end{Bmatrix} \tag{1-2}$$

Figure 1.1 shows the details of the definition of effective damage variable, and Liu assumed that only in Case 1.1-d, the unilateral effect will be presented.

Liu's model has succeeded in expressing the behavior of pure concrete under complex stress conditions. In order to apply this model to the real structures, the damage relationship between the rebar and the concrete needs to be established. In Liu's First Year Report (reference [1]), Liu developed a RC Element Damage model, which will be expressed as RCED model in this report. It is summarily introduced as following.

For simplification, only the effect along the reinforcement is considered. As shown in *Figure1.2*, it is the bond stress that enable the concrete and the re-bars to work together to resist the shearing load. The bond stress is in fact the shear stress on the bond area in the interface between the concrete and the re-bar. The bond stress is related to the relative displacement or slip, Δ, between the concrete and re-bar.

In order to provide the bond stress, there must be relative displacement (Δ) between the concrete and re-bars in the bond area. This means tat there must be some damage (slip) on the interface if loading is applied, and so the threshold of damage is zero. It should also be noted that the damage on the interface has no unilateral effect, and it is the absolute route of slip that decides the bond stress.

At first, a so-called affected zone is defined as the zone in which the slip between the re-bar and the load can cause a local damage in the concrete, shown in *Figure 1.3*. This zone includes the re-bar and the concrete around it. Hence we can treat the re-bar and the concrete within the affected zone as the RVE of the reinforced concrete. There are thus three kinds of damage in the reinforced concrete: (1) the damage, D, defined

in equal 1.1; (2) the slip on the interface between the concrete and the re-bar; and (3) the local damage in the concrete due to the slip. Of the three kinds of damage, the first and the third can be considered together using the theory given in Liu's First Year Report (reference [1]). But, the relationship between the slip and the local damage needs to be quantified by experimental test.

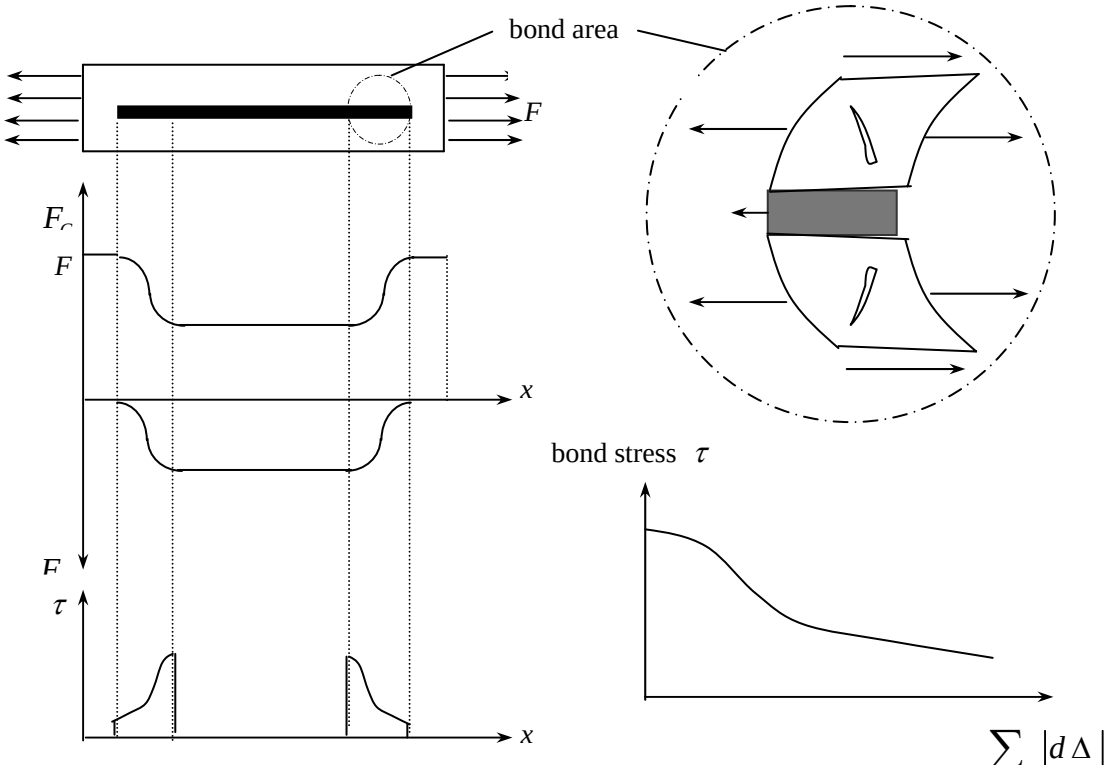

Figure 1.2 Bond area and bond stress

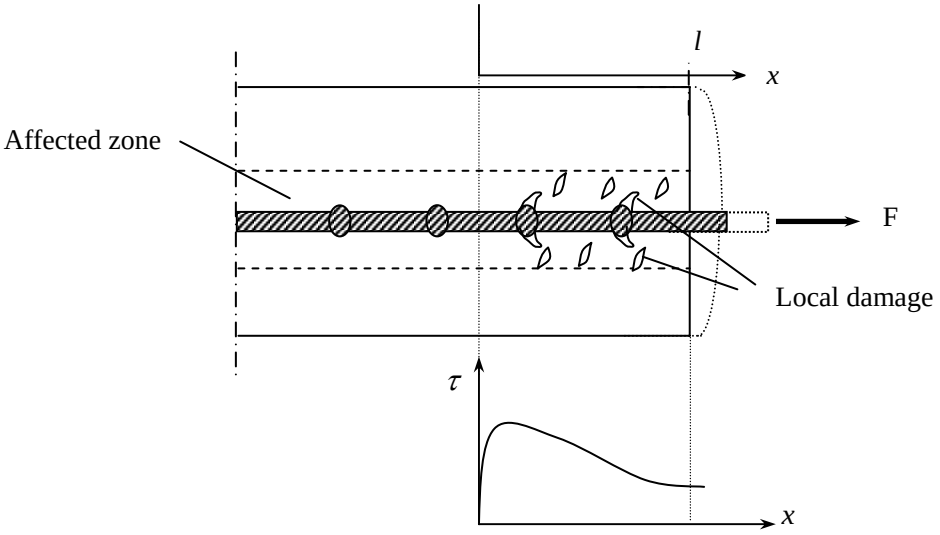

Figure 1.3 Definition of the affected zone

To consider the slip, the concrete and the re-bar can be treated separately, with special element to simulate the interface between the concrete and the steel bars. But this method needs many elements especially when many reinforcements are used. Hence, this study hopes to consider the concrete and the re-bars together, with the slip effect accounted for.

For this study, the 8-node isoparametric element is used as the basic R.C. element. To consider the local damage, two nodes (Nodes 9 and 10) are added to the element, and another two nodes (Nodes 11 and 12) are added to express the slip between the re-bar and the concrete. Nodes 9 and 11, and 10 and 12 have the same original coordinates. Each of these four nodes has just one degree of freedom, thus, its displacement is only along the rebar. Thus, the RC element has a total of 12 nodes and 28 degrees of freedom. as shown in *Figure 1.4*

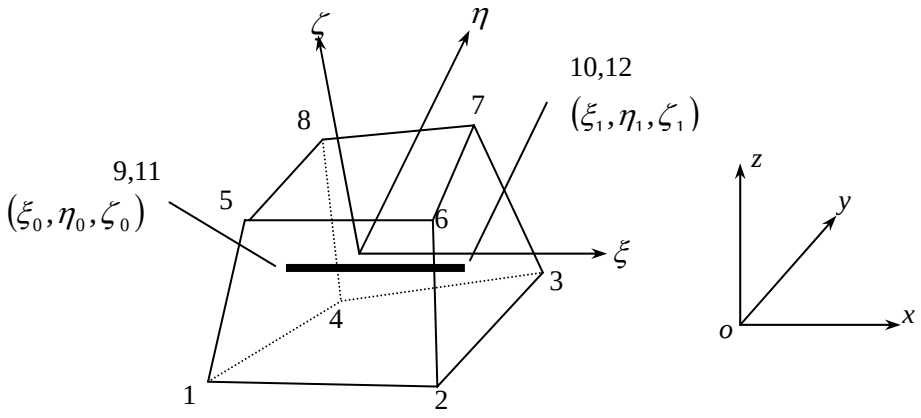

Figure 1.4 Steel bar in 8-node isoparametric element

Chapter 2 Literature Review

As stated in Chapter 1, the relationship between the slip and the local damage needs to be quantified by experimental test. Till now, the test method of the bonding stress can be divided into the following three types. That is: pull-out test of rebar, Beam-type test and uniaxial-draw test.

(1) The pull-out test.

This type of test is mainly used to test the anchoring strength of the bonding. The pull-out test can also be divided into two sub-types based on whether the transverse bar is present or not. The topical standard test specimen of the no-transverse bar pull-out test is shown as *Figure 2.1*, which is recommended by RILEM-FIP-(EB). The rebar is embedded in the concrete cube. The tension force is applied on the stretched-out end of the rebar. The protective layer is 4.5 times to the diameter of the rebar. Half of the rebar embedded in the concrete is no bonding, so as to avoid the local damage on the surface between the concrete and the blocking plate. However, when the strength of the concrete is high, it often causes the cleavage damage. So in the codes of some other countries, such as CP110, there are some transverse re-bars in the specimen, as shown in *Figure 2.2*. The China Institute of Building Science develops another type of test specimen with transverse re-bars (referring to Kang Qingliang, reference [3]). The hoop re-bars are embedded in the specimens to evaluate the influence of the transverse rebar to the bonding strength, shown as *Figure 2.3.* Several other types of specimens are developed, such as the ones shown in *Figures 2.4~2.5*, to evaluate the influence of the embedded place of the re-bars. (referring to Kang Qingliang, reference [3])

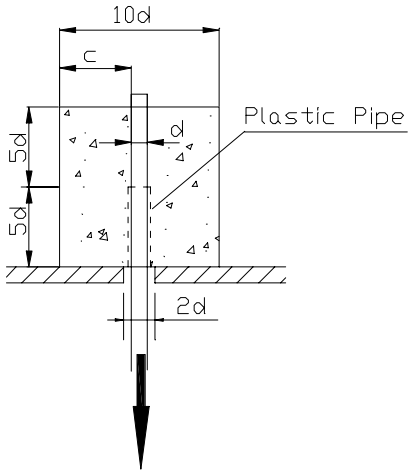

Figure 2.1 No-transverse bar pull-out test

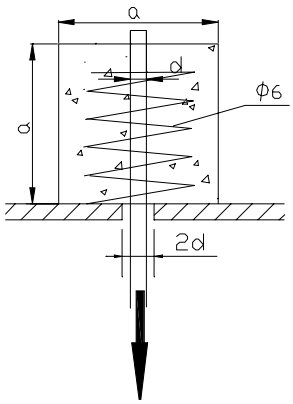

Figure 2.2 With transverse bar pull-out test

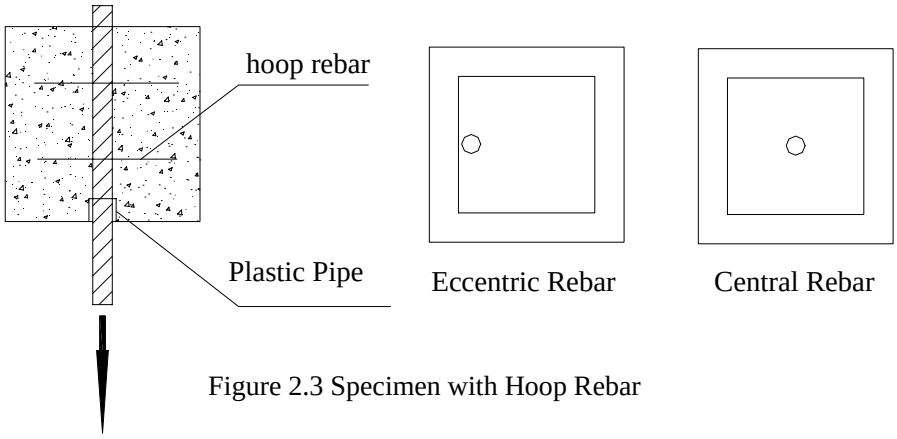

Figure 2.3 Specimen with Hoop Rebar

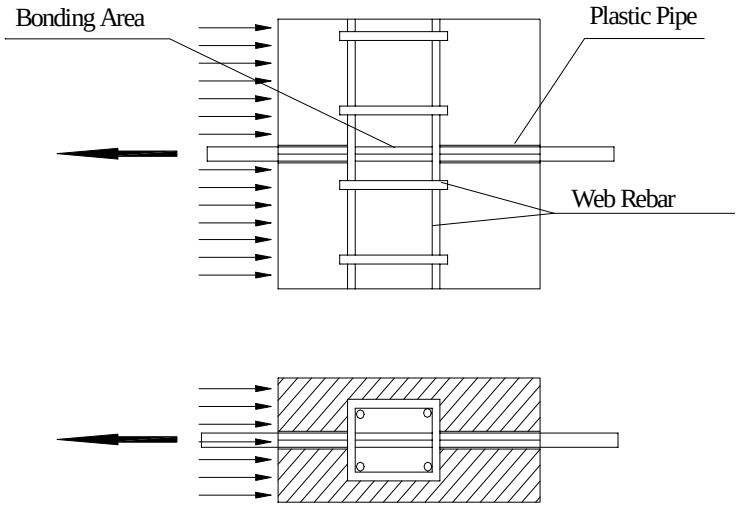

Figure 2.4 Specimen with Web Rebar

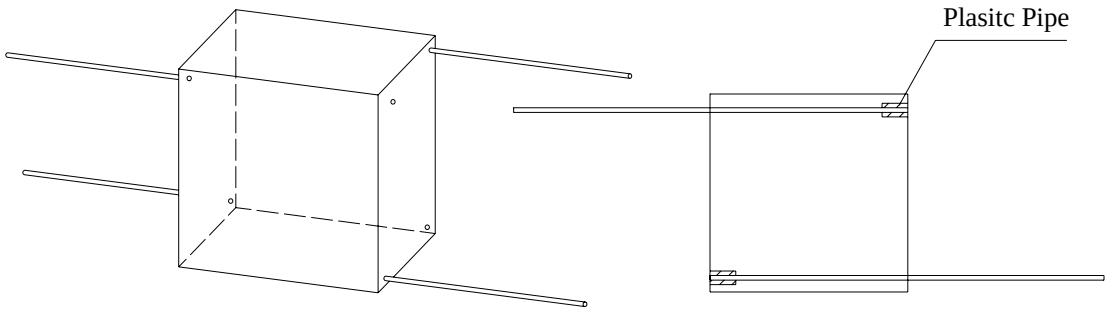

Figure 2.5 Rebar in Different places

(2) The Beam-type Test

In the real structures, there are bending moment and shearing force besides the tension force in the anchoring areas. However, for the pull-out test, on the surface between the concrete and the blocking plate, the compression stress limits the extension of the transverse crack. Hence, the beam-type bonding test is developed to simulate this real stress condition.

The beam-type bond test can be divided into two sub-types, too. One is the half beam test, as shown in *Figure 2.6* to simulate the inclined cracks. *Figure 2.7* shows are the half beam test to simulate the vertical cracks. The other type is the full beam test, as shown in *Figures 2.8 and 2.9* (referring to Kang Qingliang, reference [3]). *Figure 2.10* shows a real simply supported beam test for determining both the anchoring bond stress and the bond stress between the cracks.(referring to Song Yupu, reference [7]).

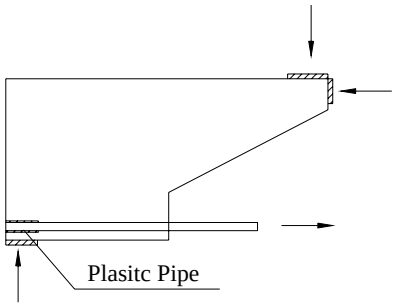

Figure 2.6 Half-beam Test to Simulate the Inclined Crack

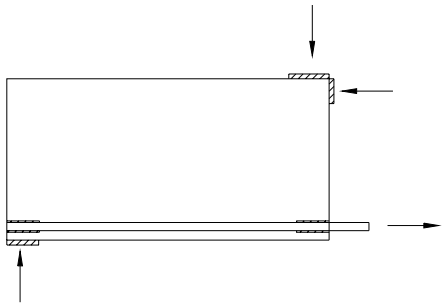

Figure 2.7 Half-beam Test to Simulate the Vertical Crack

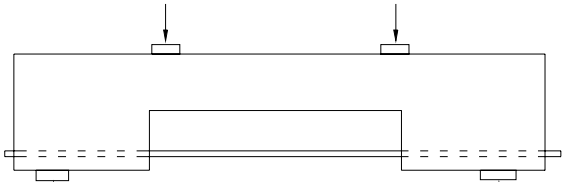

Figure 2.8 Half-beam Test to Simulate the Inclined Crack

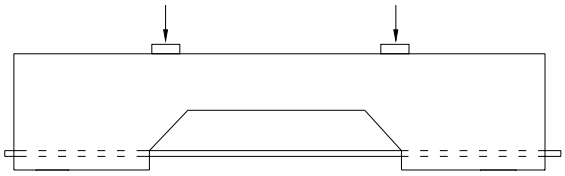

Figure 2.9 Half-beam Test to Simulate the Vertical Crack

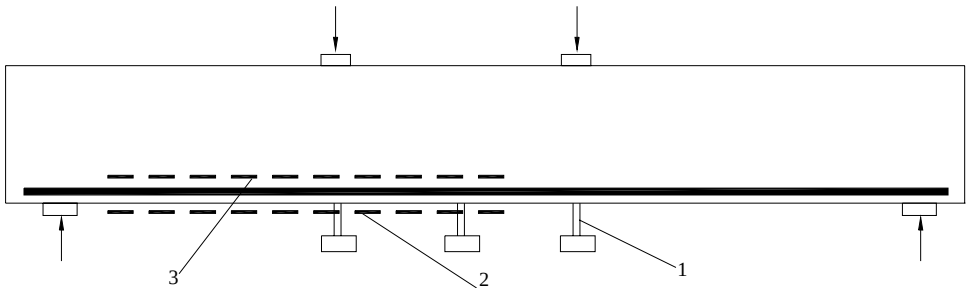

Figure 2.10 Simply Supported Beam Test

1: Lever-type Strain Gauge 2: Strain Gauge On the Bottom

3: Strain Gauge on the Side

(3) Uniaxial-draw Test

As the specimens of the beam-type bond test are much more complex, the

uniaxial-draw test is developed to simulate the stress-state between the pure bending cracks. The *Figure 2.11* displays the topical uniaxial-draw test. (referring to Kang Qingliang, reference [3])

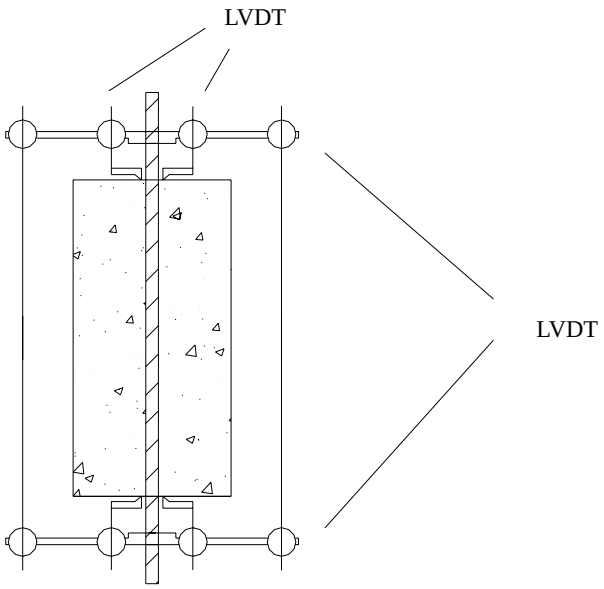

Figure 2.11 Uniaxial-draw Test

Although there are many test methods available to study the bond between the concrete and the steel bar, in the real life structures, the bonding states are much more complex than the test conditions. Thus, new bond test method still needs to be developed.

Chapter 3 Experiment Procedure

§ 3.1 The Purpose of the Experiment

In the damage evolution equation of RCED model (referring to Liu Yu, reference [1]), the local damage caused by slip can be assumed to be

$$D_l = a_1 D_s \vec{n}_1 \otimes \vec{n}_1 + a_2 D_s \left(\vec{n}_2 \otimes \vec{n}_2 + \vec{n}_3 \otimes \vec{n}_3 \right) \tag{3-1}$$

where the parameters a_1, a_2 are used to describe the degree of local damage around the re-bar. When the re-bar is pulled out, D_s is assumed to be 1. Then, comparing the elastic module of the concrete before and after test, the two parameters can be determined. The elastic module variance of the concrete around the re-bar is to be obtained through the test.

According to RCED model, the total bond force can be written as

$$F_b = \frac{l}{2} K_s \left(1 - D_s\right) \cdot \left(\Delta_1 + \Delta_2\right) \tag{3-2}$$

Through the test, the evolution rule of D_s can be obtained by fitting a $F_b - \Delta$ curve, as shown in *Figure* 3.1.

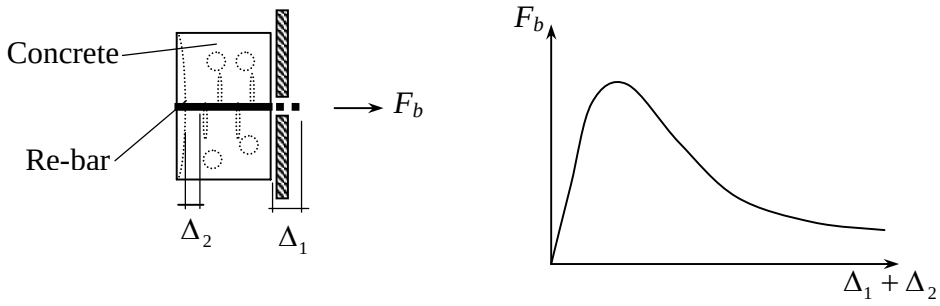

Figure 3.1 Evolution of the slip damage

Where F_b is the tensile load act on the re-bar and Δ_1, Δ_2 are the relative displacement between re-bar and concrete on the top and bottom surface, respectively.

The size of the local damage zone caused by the re-bar slip also needs to be determined from the experiment. Then the reasonable size of the reinforced concrete element can be set

for the finite element analysis.

In RCED model, the deformation of the bond zone between the concrete and the re-bar is assumed to be pure shear deformation, just as described in Chapter 2. But till now, none of the bond tests can precisely describe the assumption and boundary conditions of RCED model. So a new bond test method should be designed to obtain the data needed.

§ 3.2 Device and the Method of the Experiment

In order to satisfy the assumption in RCED model, a new method is designed to test the bond strength. The specimen is as shown in *Figure 3.2*. The concrete specimen is cylindrical in sharp, with the steel bar embedded along the central axis. The specimen is rounded in a PVC pipe. Special glue is used to stick the pipe to the surface of the concrete. The loading device is as shown in *Figure 3.3.* A hole is made in the center of a thick steel plate. The radius of the hole is exactly equal to the radius of the concrete specimen. The steel plate is fixed to the base of the tension machine – Instron 4486. The steel bar is then clamped to the tension machine so as to exert an upward pull on the rebar. However, the steel plate will hold back the PVC pipe so as to stop the specimen from moving with the re-bar. In this way, a constraint force is applied to the concrete through the PVC and the glue. The load transmission in the whole process is from the clamping device to the steel bar, to concrete through the bonding, to the glue, to the PVC pipe, and then to the base of the tensile test machine through the steel plate. The force applied on the specimen is as shown in *Figure 3.4*. The deformation of the concrete is pure shear deformation. Till now, In RCED model, the influence of the circumferential pressure to the bonding damage has not been considered. So in this test, the PVC pipe is split into 6~12 segments to let the concrete expand freely. The whole specimen satisfies RCED model precisely and the results of the tests can be used to verify the model.

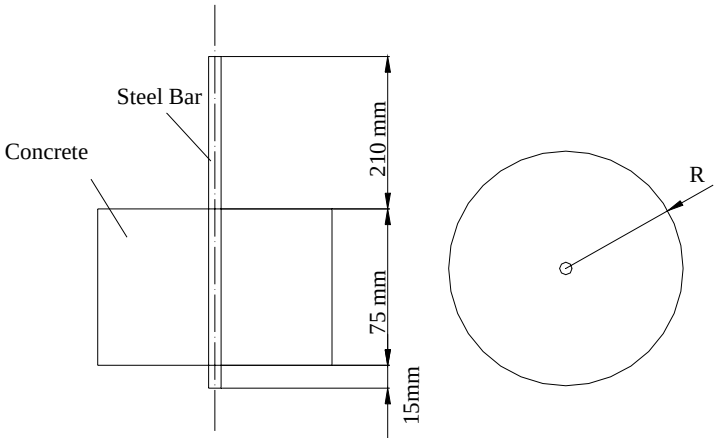

(a) Elevation (b) Plan

Figure 3.2 Specimen

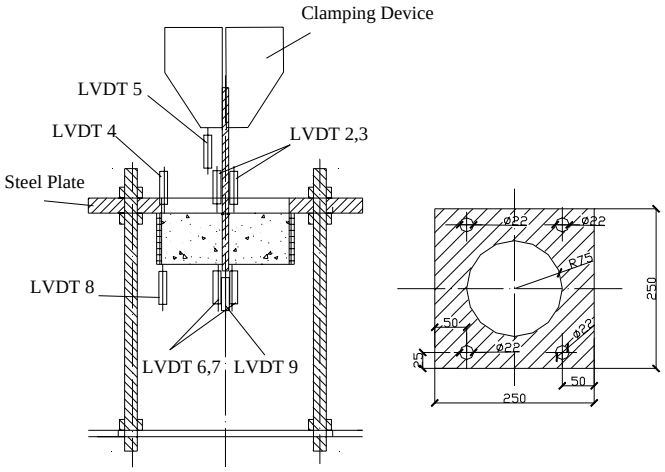

Figure 3.3 Loading Device

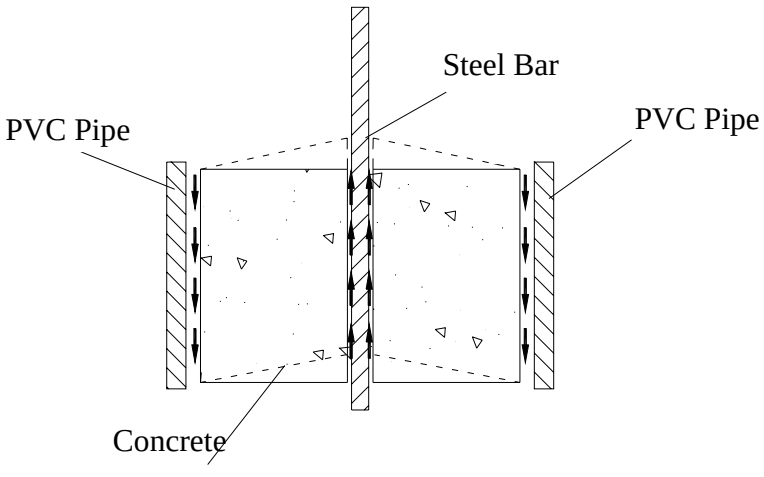

Figure 3.4 Stress State of the Specimen

In order to permit a more exactly distributed shear deformation of the concrete, the specimen should not be too thick. Hence, the height of the specimen is set to about 7.5 cm. The biggest diameter of the coarse aggregate is d=2 cm, so the thickness is greater than 3d. Thus the concrete can be treated as an isotropic material. The ingredients of the concrete mixture are listed in Table 3.1.

Table 3.1 The Ingredients of the Concrete Mixture

Material	Cement	Water	Fine Aggregate	Coarse Aggregate
Weight (kg)	40	30	60	120

The diameters of the specimens are 5 cm, 10 cm, 15 cm, 20 cm, and 30 cm to investigate the influence of the size of the element. All the steel bar are ϕ10 crescent rib steel bar, so that the results of different specimens are comparable. The material parameters of the steel bar are shown in Table 3.2.

Table 3.2 Material Parameters of the Steel Bar

Min Proportion Stress	Min Yielding Stress	Min Fracture Stress
400 Mpa	500 MPa	600 MPa

Because the surface of the concrete around the steel bar often cracks or peels, influencing the measurement of the LVDT, we placed 2 LVDTs on the top and the bottom surface of the concrete around the steel bar. The relative displacement between LVDT 2, 3 and LVDT 5 is Δ_1. The relative displacement between LVDT 6, 7 and LVDT 9 is Δ_2.The relative displacement between LVDT 2, 3 and LVDT 4 is δ_1. The relative displacement between LVDT 6, 7 and LVDT 8 is δ_2. The test is under displacement control so that the full $F_b - \Delta$ curve can be obtained to determine the evolution rule of the damage parameter D_s.

Comparing the variation of δ_1, δ_2 with the diameter of the specimen, we can obtain the influence of the size of the specimens. Before and after the test, using ultrasonic wave to determine the concrete elastic module of the damage area and to measure the crack distribution on the fracture surface, we can obtain the size of local damage zone caused by the slip.

Figure 3.5 shows the specimen before test. In order to improve the adhesive strength between the concrete and the glue, the surface of the specimen is roughened with hand grinder. The inner surface of the PVC pipe is also roughened and is split into several segments to eliminate the circumferential confinement effect. Several millimeters of the pipe are left uncut so that when the pipe is glued to the concrete, the top edge is kept even, and the reaction force from the steel plate is distributed evenly along the circumference. The result of the experiment shows that circumferential confinement effect is very small.

The test setup is shown as *Figure 3.6*. The steel plate is fixed to the base of the test machine by four ϕ20 steel columns, whose cross section area is 1256 mm^2, which is 16 times to the cross section of the re-bar which is 78.5 mm^2. The stiffness of the loading device is much larger than the specimen, so we can treat the loading device as rigid.

(a) Concrete Specimen before Test

(b) PVC Pipe before Test

(c, d) During the Test

Figure 3.5 Specimen Before and During Test

The test setup is as shown in *Figure 3.6*. The steel plate is fixed to the base of the test machine by four $\Phi 20$ steel columns, whose cross section area is 1256 mm^2, and is 16 times the cross sectioned area of the re-bar which is 78.5 mm^2. The stiffness of the loading device is much larger than the specimen, so we can treat the loading device as rigid.

In the whole force-transmit-path, the glue is the most important component. Sikadur 31(referring to Sikadur 31 manual, reference [11]) is selected for our test. It can adhere concrete, plastic, as well as steel. The compressive strength is higher than 70 MPa, The flexural strength is higher than 36 MPa, the tensile strength is higher than 14.8 MPa and the Shear Strength is higher than 21 MPa. According to the bonding stress empirical formula of Tsinghua University, (referring to Teng Zhiming, reference [5])

$$\tau = (61.5d - 693d^2 + 3.14\times10^3 d^3 - 0.478\times10^4 d^4) f_{ts} \sqrt{c/\phi}\psi(x) \qquad (3\text{-}3)$$

where d is the slip of the steel bar. f_{ts} is the fracture strength of concrete. c is the thickness of the protect layer. ϕ is the diameter of the steel bar. x is the distance to the end of the specimen.

The bonding strength between the concrete and the steel bar should be about 10 MPa. So the maximum shear stress that acts on the glue is about 2 Mpa, which is less than 21 MPa. So Sikadur 31 can be applied in our test.

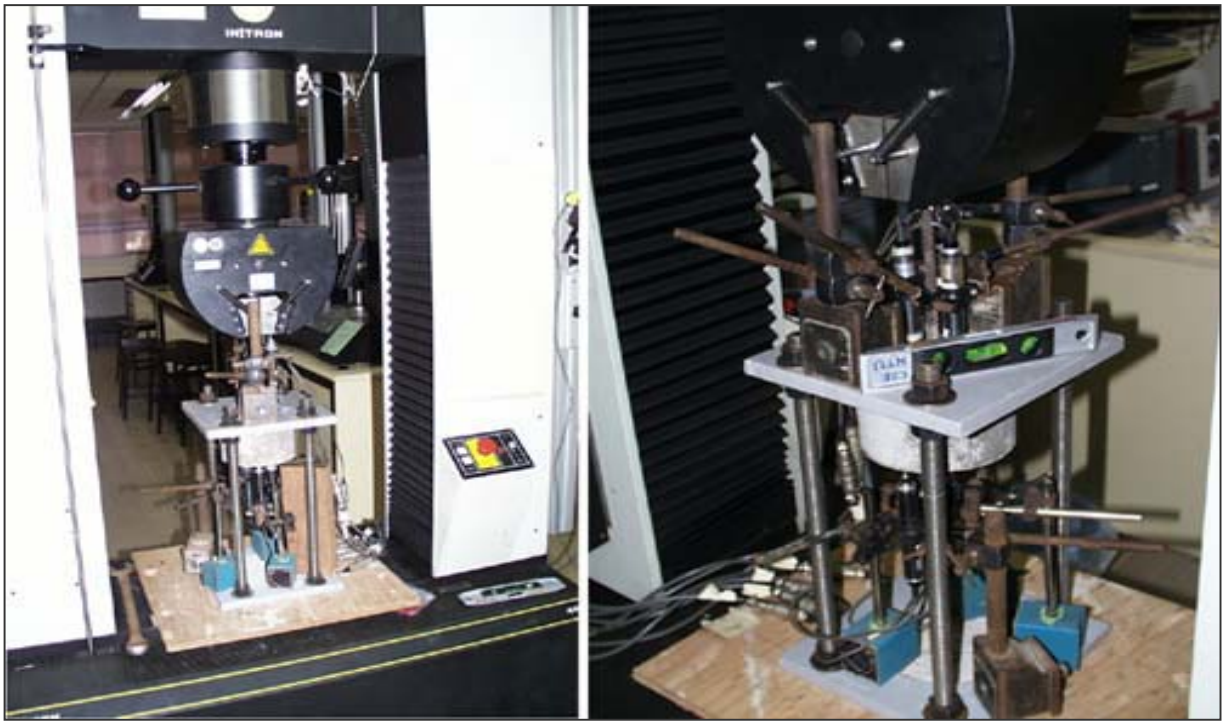

Figure 3.6 Test Device Setup

The test machine is the Instron model 4486 universal test machine, with a tensile capacity of 300 kN. From equal 2-3 the maximum bond stress is about 10 Mpa, and the maximum bond force should be about 22.4 kN, which is less than the machine capcity of 300 kN. The LVDTs on the top of the specimen can measure up to 10 mm, and those on the bottom are up to 25 mm. The accuracy is 0.001 mm and 0.002 mm, respectively.

§ 3.3 Test procedure

1. Design of the Mold

Because the sizes of the specimens are uncommon, the mold of the specimen must be specially designed. The mold should be able to easily hold the re-bar in place during casting of the concrete and easy to use. The mold is shown in *Figure 3.7*

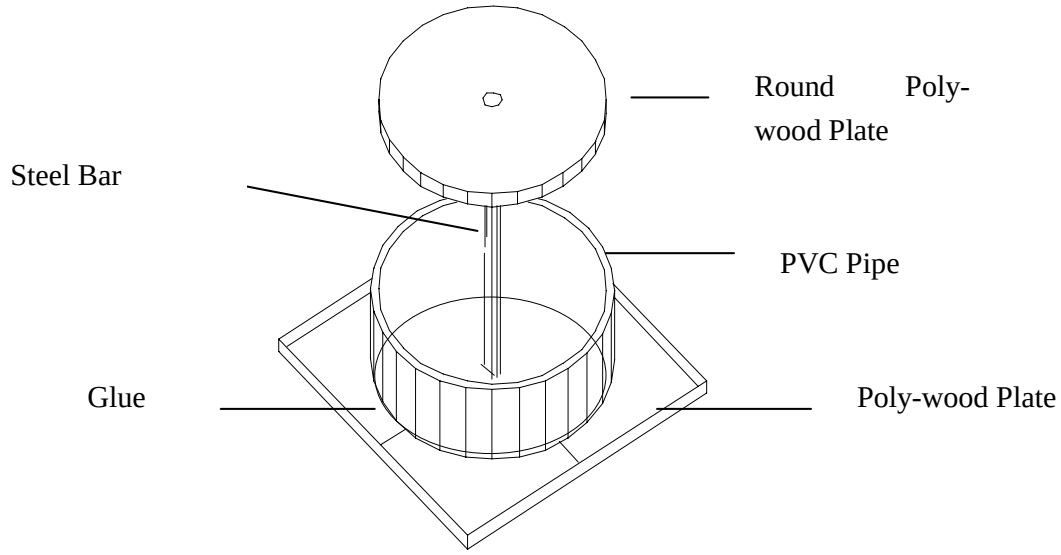

Figure 3.7 Specimen Mold

The main body of the mold is a piece of PVC pipe. It is not only used as the mold for the concrete, but also for transferring the load. A square poly-wood plate is adhered to the bottom of the PVC pipe with glue. A 9-mm hole is made in the center of the poly-wood plate. The steel bar is hammered into the hole. Another round poly-wood plate is used as the cover whose diameter is equal to the internal diameter of the PVC pipe. An 11-mm hole is made in the center of the plate. The steel bar goes through the hole and the round plate is covered on the top of the concrete. The steel bar is then fixed firmly along the central axis and it will not move when the concrete is being vibrated.

2. Test of Steel Bar

In the test, the steel bar is fixed on the clamping device of the tensile test machine. LVDT 5 measures the displacement of the clamping device. It is the sum of (1) the relative displacement between the steel bar and the concrete, (2) the elongation of free part of the steel bar and the slip between the steel bar, and, (3) the clamping device. In order to know the material characteristics of the steel bar and analyze the influence of the slip between the

steel bar and the clamping device, we test the steel bar is tested first. The test device is shown in *Figure 3.8*. The stress-strain curve of the steel bar is shown in *Figure 3.9*. The equivalent elastic module when load is lower than 30 kN is what we need to calculate the equivalent deformation of the steel bar, which is shown in *Figure 3.10*. It is apparant that because of the slip between the clamping device and the steel bar, the equivalent elastic module is much lower than the normal value. The equivalent elastic module of the steel bar is about 66Gpa, which is 1/3 of the ordinary elastic module.

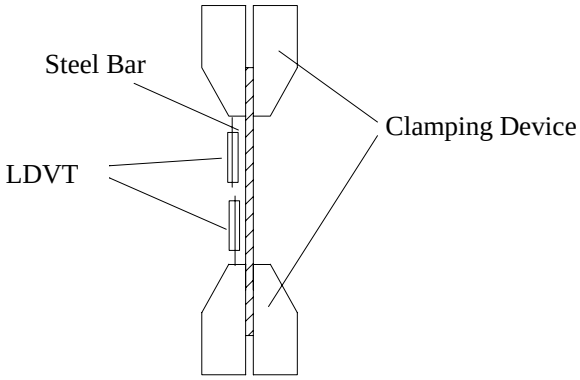

Figure 3.8 Steel Bar Test

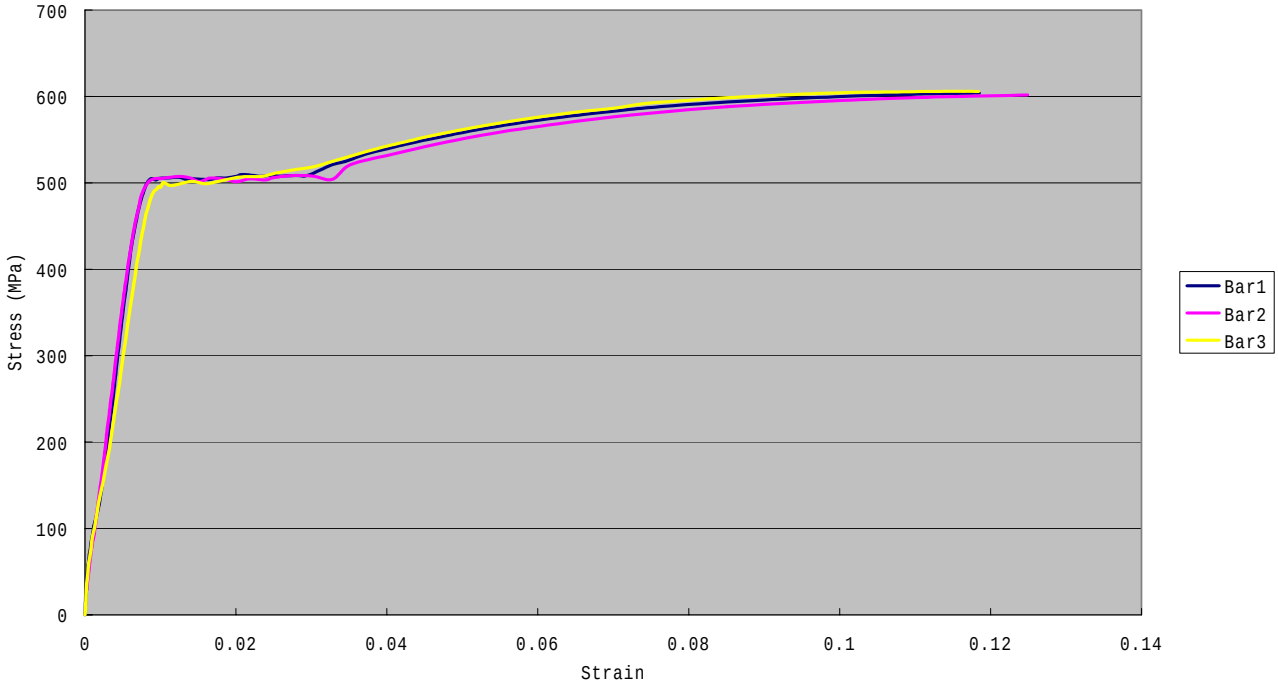

Figure 3.9 Stress-Strain Curve of Steel Bar

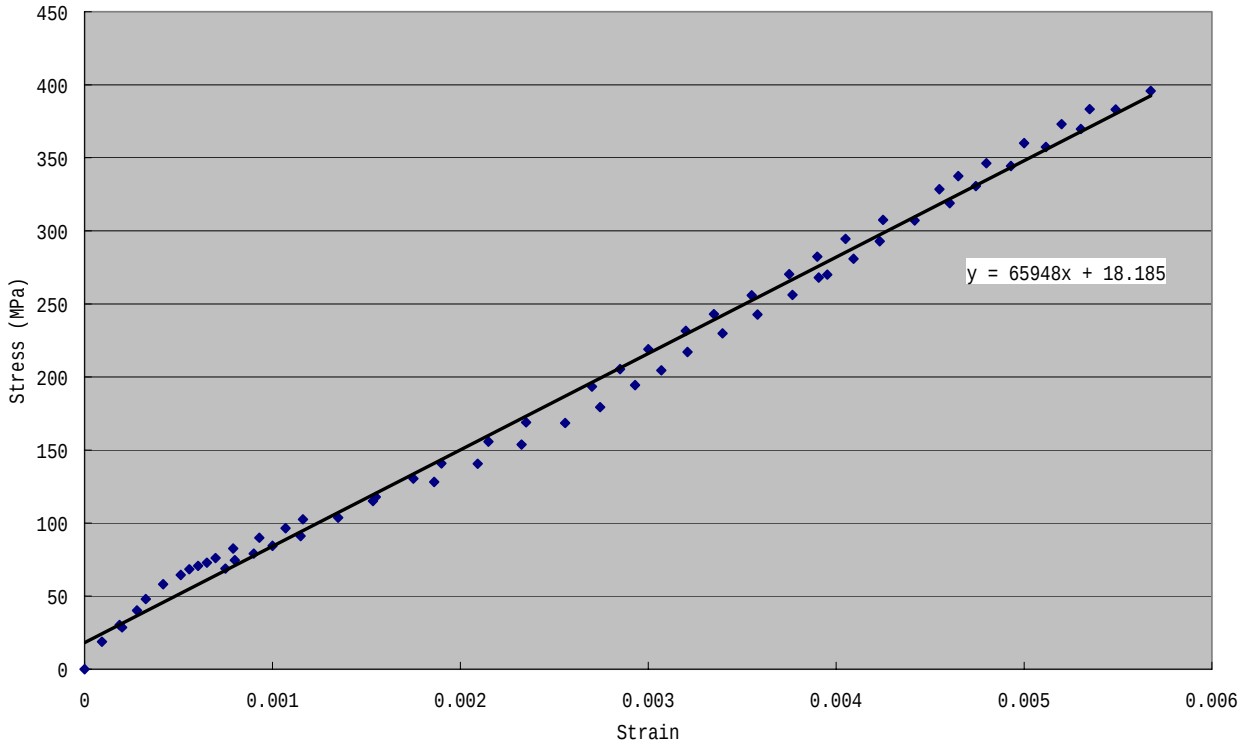

Figure 3.10 Equivalent Elastic Module of Steel Bar

3. Casting of Concrete

In order to obtain consistent specimens, all the concrete is mixed and cast at one go. Because the vibration-table isn't big enough to vibrate all the specimens at the same time, a standard specimen is made each batch. In order to let strip the mold easily, oil is spread on the internal surface of the mold. All together, 36 specimens are produced and listed as Table 3.3.

Table 3.3 List of Test Specimens

Specimen Type	ϕ5 cm	ϕ10 cm	ϕ15 cm	ϕ20 cm	ϕ30 cm	15cm standard tube	15cm standard cylinder
Number	4	7	7	7	5	3	3

The mold is removed 36 hours after casting. The specimens are cured in the curing room of Heavy Structures Lab. The curing period is 28 days.

4. Design of the Loading Device

The design and setup of the loading device is as shown in *Figure 3.3*.

5. Specimens Analysis before Test

In order to ascertain the quality of our specimens, we use UPV to test the specimens along the radial axis after the curing period, as shown in *Figure 3.11*, so as to determine the dispersion rate of the concrete strength. The test result is as shown in *Figure 3.12*. We found that the UPV value of the Specimen 20-3 is much larger than that of the others, indicating that there may be some inner damages in the specimen. The final test result proved this suspicion to be true.

6. Trial Loading and Analysis of Failure

When all the preparative work is completed, a trial loading is first tested on Specimen 5-2. We found that after the load is applied, there is slip between the concrete and the PVC pipe, which implied that the strength of the glue between the concrete and the PVC pipe is not strong enough. The glue is destroyed when the load reached 13.6 kN.

Specimen 10-7 is then tested as the second trial loading. The failure is still due to the glue when load reaches 23.7 kN. The specimen is stuck in the hole of the steel plate after it is pull out from the PVC pipe. Because it is circumferential firmly constrained by the plate, at last the failure load of bonding reaches 38.1 kN. The upper surface of the concrete fails with tapering shape, as shown in *Figure 3.13*. The steel bar is pulled out. But there is no longitudinal cracks happen, as shown *Figure 3.14*.

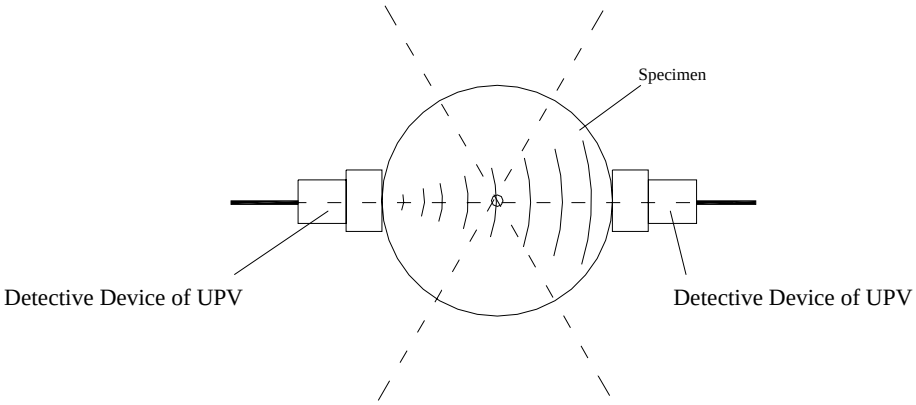

Figure 3.11 Testing the Specimen with UPV

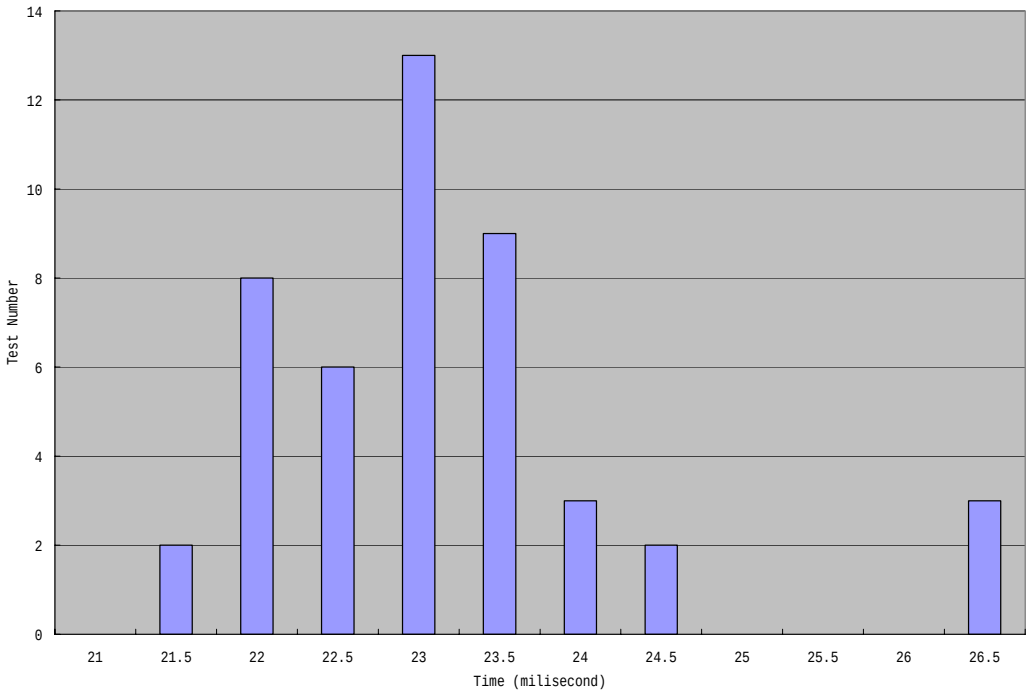

Figure 3.12 UPV Test Result

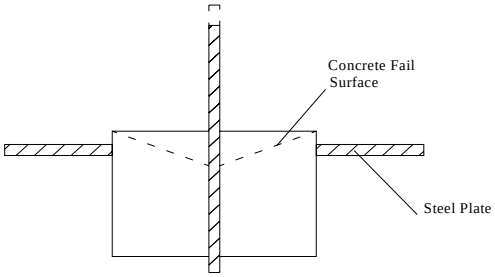

Figure 3.13 Fail Surface of 10-7

Figure 3.14 Test Result of Specimen 10-7

Then we tried applying load in a different way: We used the steel plate to stop the specimen directly, without the PVC pipe, as shown in *Figure 3.15*. We tested Specimen 10-1 in this way. The result is satisfactory and the peak load achieved is 21.19 kN.

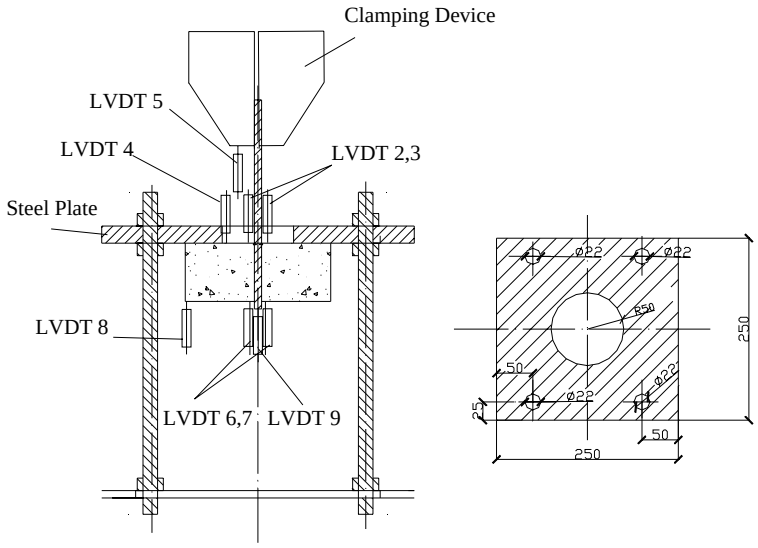

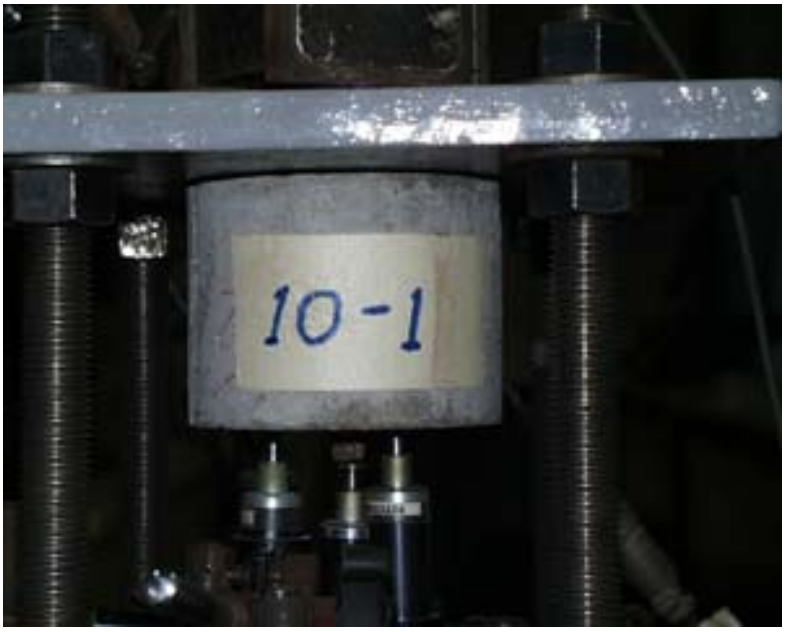

Figure 3.15 Load Applied directly without PVC Pipe

So we made the following conclusions:

(1) Comparing Specimen 10-7 and 10-1, we think the strength of the glue can satisfy the requirement, because the bond of Specimen 10-1 fails at 21.19 kN while the glue of Specimen 10-7 fails at 23.7 kN. The reason for failure of glued interface may be that we did not process the adhesive surfaces properly.

(2) The influence of the circumferential confinement is very obvious, which causes the bond of Specimen 10-7 fails at 38.1 kN. For Specimen 5-2 and 10-7, we just cut one gap in the PVC pipe. The practice shows that it is not enough. The circumferential confinement is still very large.

7. Improving the Method

From the experience we earned during the trial test, we carried out the following improvement to the method.

(1) We use sand grinder to deeply roughen the inner surface of the PVC pipe. The depth of

the roughness is about 2 mm to enable the mechanical bite force to be exerted completely.

(2) The surface of the concrete is roughened with hand grinder, too.

(3) Split the PVC pipe finely. The ϕ10cm PVC pipes are split to 6 segments, the ϕ15 ones are splited into 8, and the ϕ20 and ϕ30 ones are split into 12 segment to eliminate the circumferential confinement.

8. Formal Loading

Using our improved test method, we first tried out on Specimens 15-5 and 10-5. The result is just as expected. The glue worked very good and the specimen failed at the bond between the concrete and the steel bar. The deformation and the failure shape conformed to the theoretical analysis.

The following *Figures 3.16* to *3.23* show the major failure shape of the specimens. All the failure modes of the specimens are cleavage failure. The process of the failure is such: firstly, when the load approached the peak point, the radial cracks appeared on the top surface of the concrete around the steel bar. The cracks extended very fast. Soon they ran through the top surface and extended downwards along the side of the specimen. At the same time, the stiffness of the specimen decreased quickly and when the cracks ran through the top surface, the load came to the peak. The cracks extended so fast that the process was not able to be record. The speed of the downward crack extension varied for different specimens. Generally, the larger the specimen, the higher the bonding strength and the quicker the cracks extended. The failures of Specimens 10-4, 15-4 and all most all of the specimens whose radius is larger than 20cm are pure brittle failure, without softening phase. Because Specimen 20-3 has original internal damage, the ultimate load is much lower than other’s, and the softening stage is obtained. The cracks reached the bottom of the specimen and even went through it. Some specimens directly split after that and fell down from the load cell. Before and after the load application, we use UPV to test the module of the concrete.

Figure 3.16 Specimen 10-1 after Test

Figure 3.17 Specimen 10-4 after Test

Figure 3.18 Specimen 10-5 after Test

Figure 3.19 Specimen 15-1 after Test

Figure 3.20 Specimen 15-5 after Test

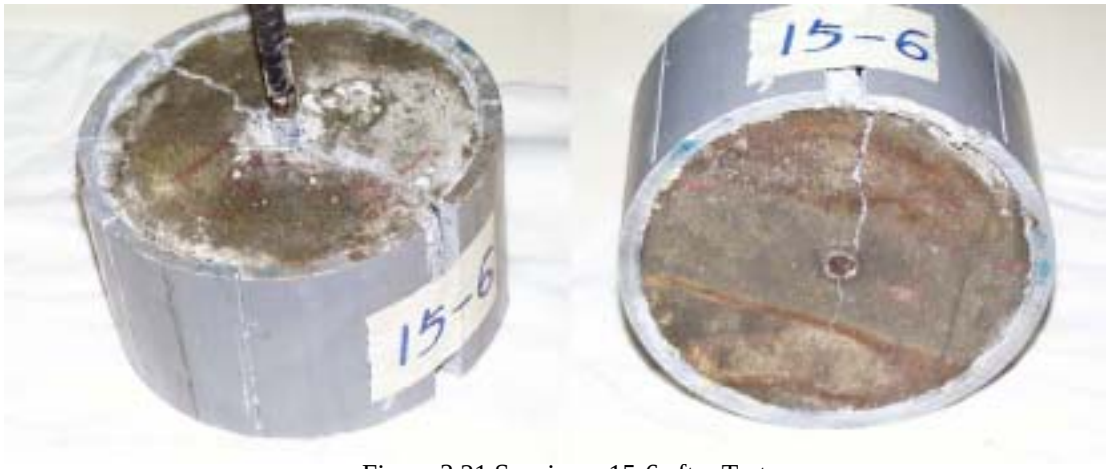

Figure 3.21 Specimen 15-6 after Test

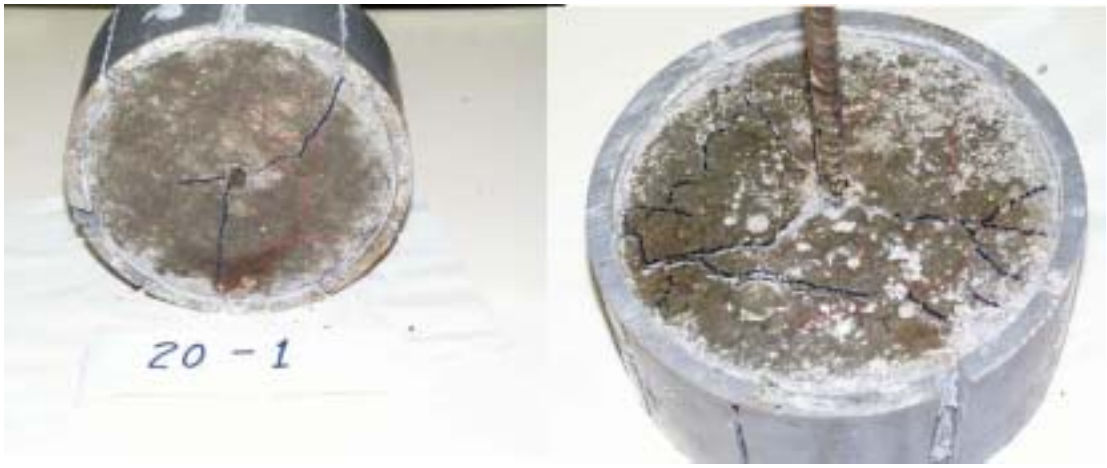

Figure 3.22 Specimen 20-1 after Test

Figure 3.23 Specimen 20-5 after Test

9. Standard Specimen Test

Standard specimen test has also been carried out to verify Liu's concrete model(referring to Liu's Fist Year Report, reference [1]), and to obtain the strength and elastic module of the concrete that we cast.

(1) Standard Tube Specimen

Three 15×15×15cm standard tube specimens are tested. The test result is as shown in Table 3.4.

Table 3.4 Test Result of Standard Tube Specimens

Specimen Number	1	2	3
Max Load (KN)	953	1061	959
Max Strength (MPa)	42.36	47.16	42.62

The average strength of f_{cu} is 44.047 MPa.

(2) Standard Cylinder Specimen

Strain gauges are set on every cylinder specimen, as shown in *Figure 3.24*. Load is applied through constant displacement. The longitudinal stress-strain curve, lateral stress-strain curve and stress-Poisson's ratio curve are shown in *Figures 3.25, 3.26*, and *3.27*, respectively.

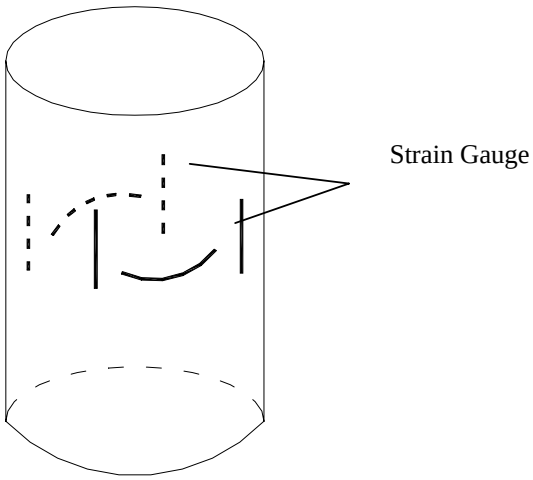

Figure 3.24 Six Strain Gauges on Standard Cylinder Specimen

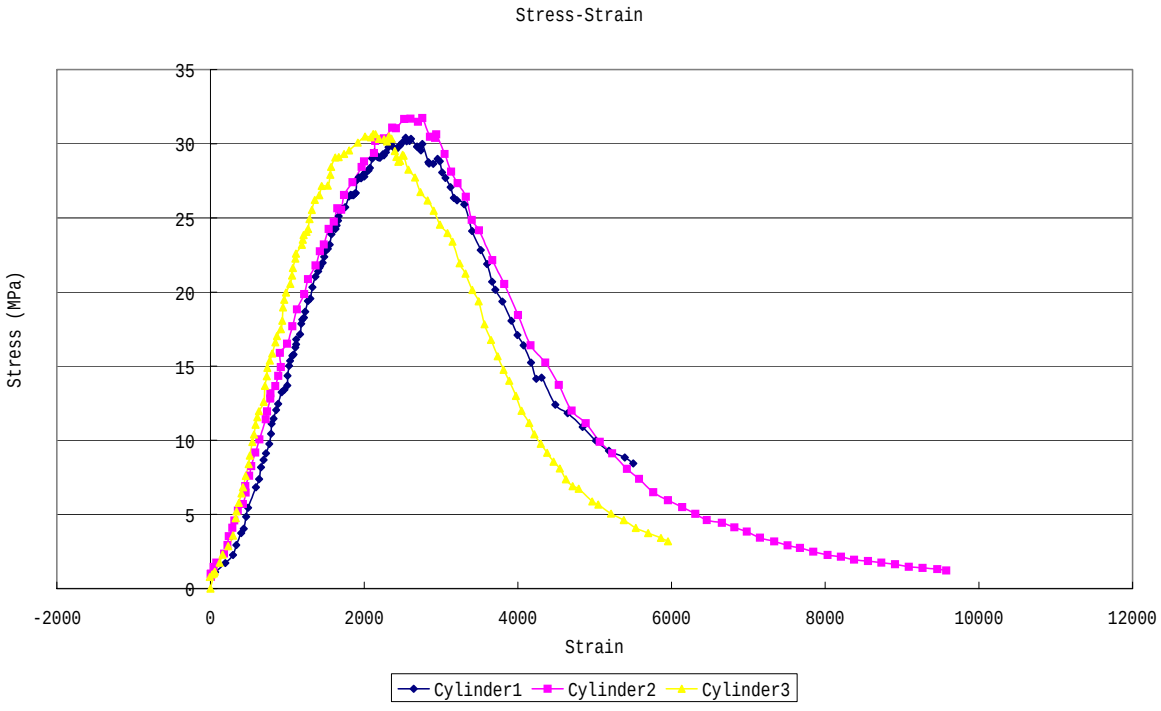

Figure 3.25 Lognitudinal-stress-strain Curve

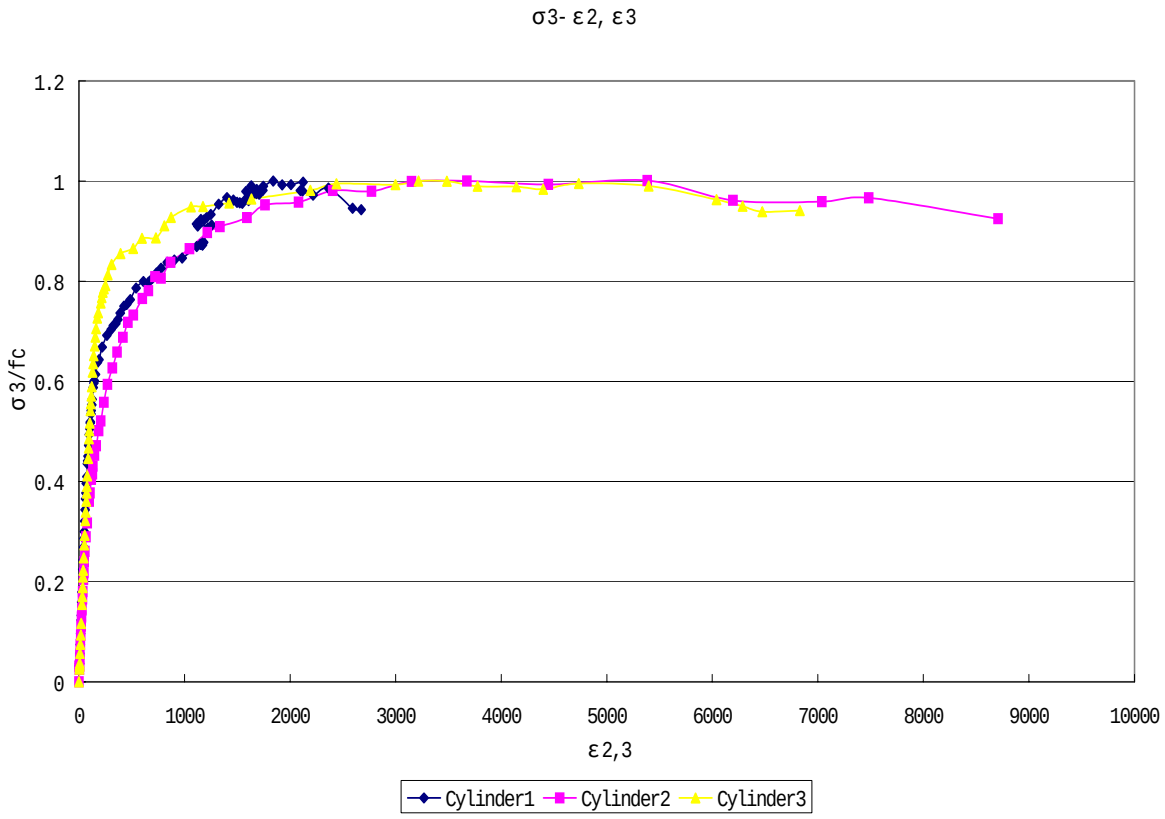

Figure 3.26 Side-Stress-Strain Curve

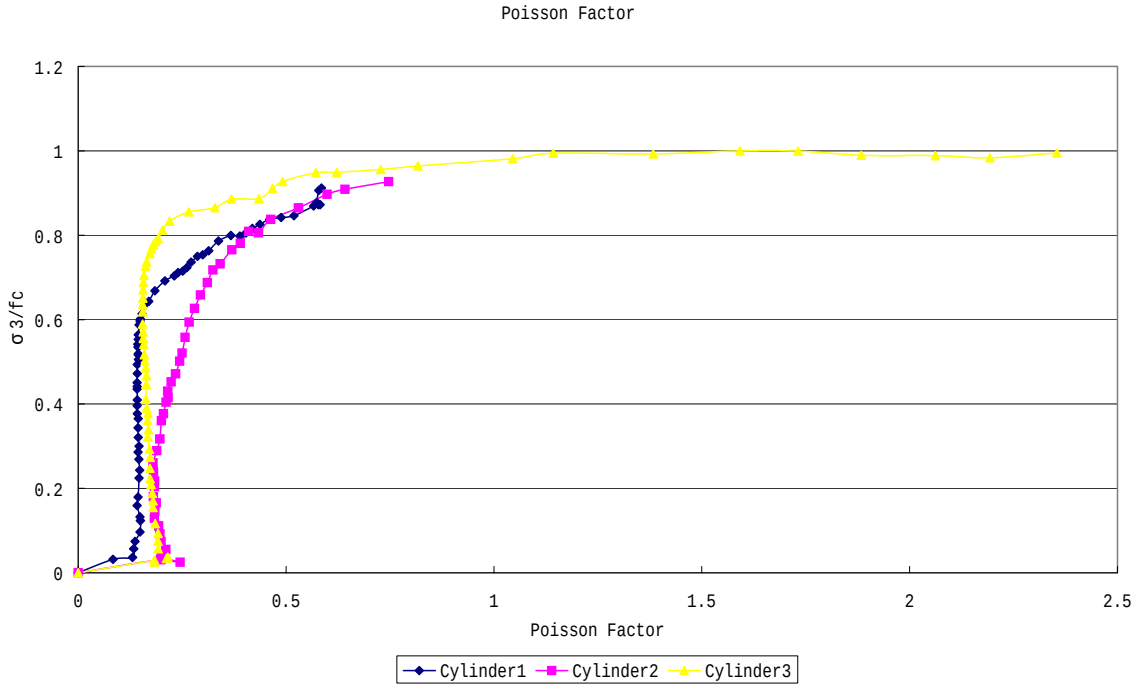

Figure 3.27 Stress-Poisson Ratio Curve

Chapter 4 Experimental Data Analysis

§ 4.1 Original Experiment Data

Shown in *Figures 4.1* and *4.2* are the two groups of typical original test curves of Specimen series 10 and 15. “Top Center” refers to the displacement of the concrete around the steel bar on the top surface of the specimen. “Top Edge” refers to the displacement of the edge of the top surface. “Top ST” refers to the displacement of the steel bar on the top. So do the same for “Bottom Center”, “Bottom Edge”, and “Bottom ST”.

§ 4.2 $\tau - \Delta$ Curve and Curve Fitting

Figures 4.3, 4.4, 4.5, and *4.6* are the $\tau - \Delta_1 + \Delta_2$ relationship of Specimen Series 10, 15, 20, and 30, respectively. τ is the average shear stress. Δ_1 is the relative displacements of the steel bar and concrete on the top surface. Δ_2 is the relative displacements of the steel bar and concrete on the bottom surface.

Because Specimen Series 10 and 15 have stable softening stage, we choose them to do the curve fitting. We found that the damage process of the two curves can be fitted by one function. That is

$$\tau = \frac{0.7260\tau_{\max}(\frac{\xi}{\xi_0}) + 0.061(\frac{\xi}{\xi_0})^{3.2}}{1 - 0.916(\frac{\xi}{\xi_0}) + 0.642(\frac{\xi}{\xi_0})^{2.87}} \tag{3-1}$$

where ξ_0 is the displacement at the peak point.

Results of curve fitting are shown in *Figures 4.7, 4.8.* This is the damage evolution rule of D_s, which is used in Equal 3-2.

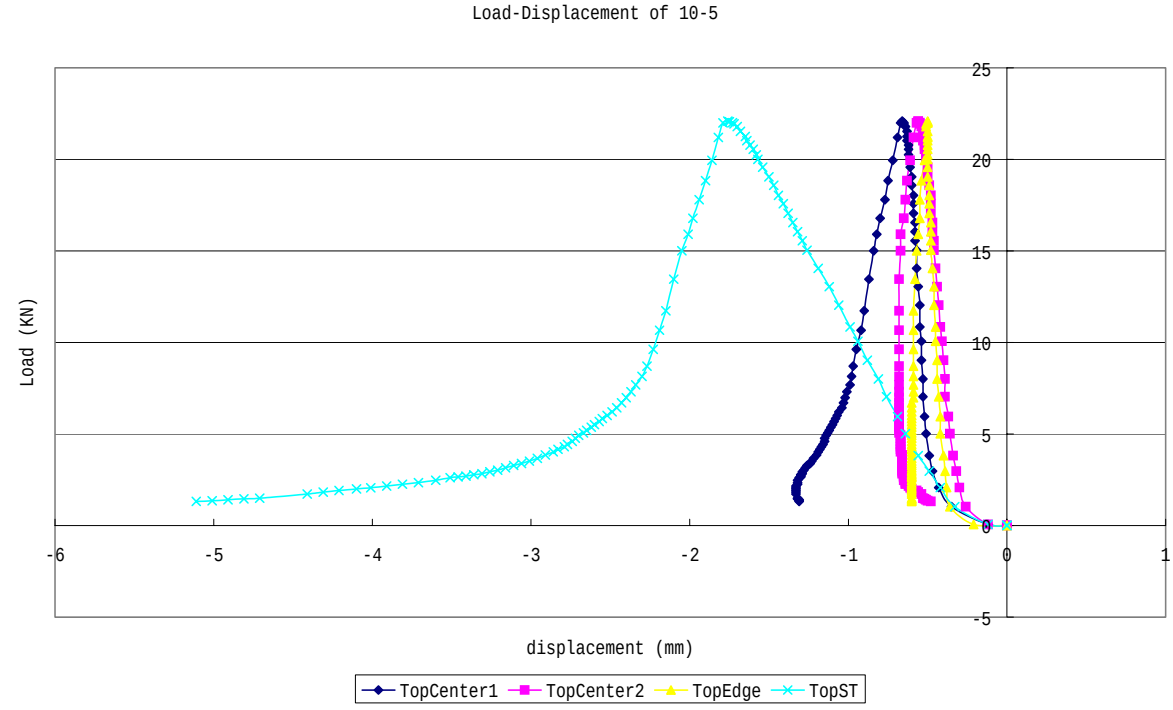

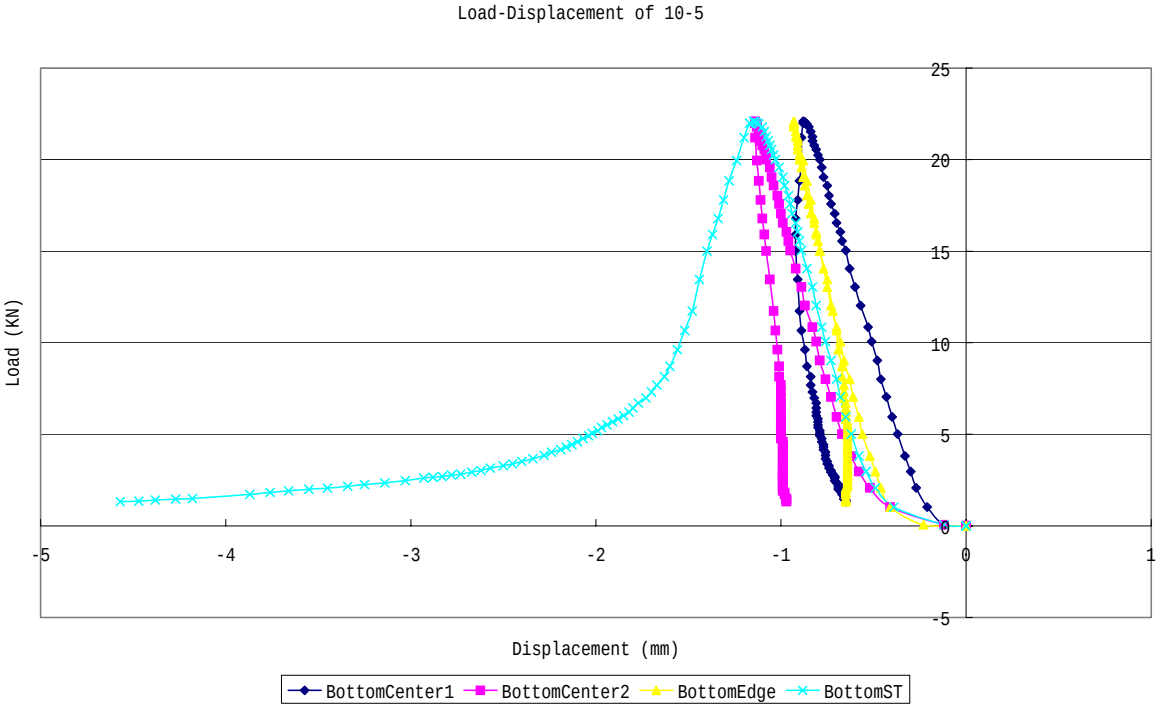

Figure 4.1 Original Data of Specimen 10-5

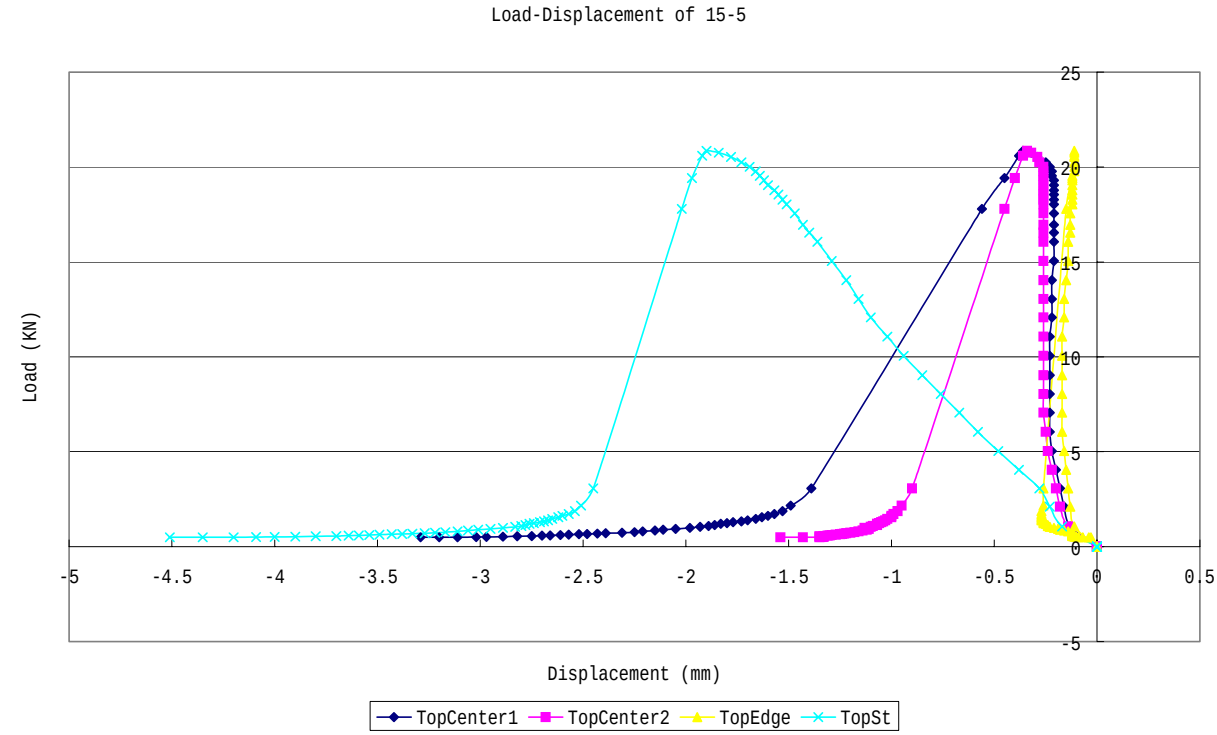

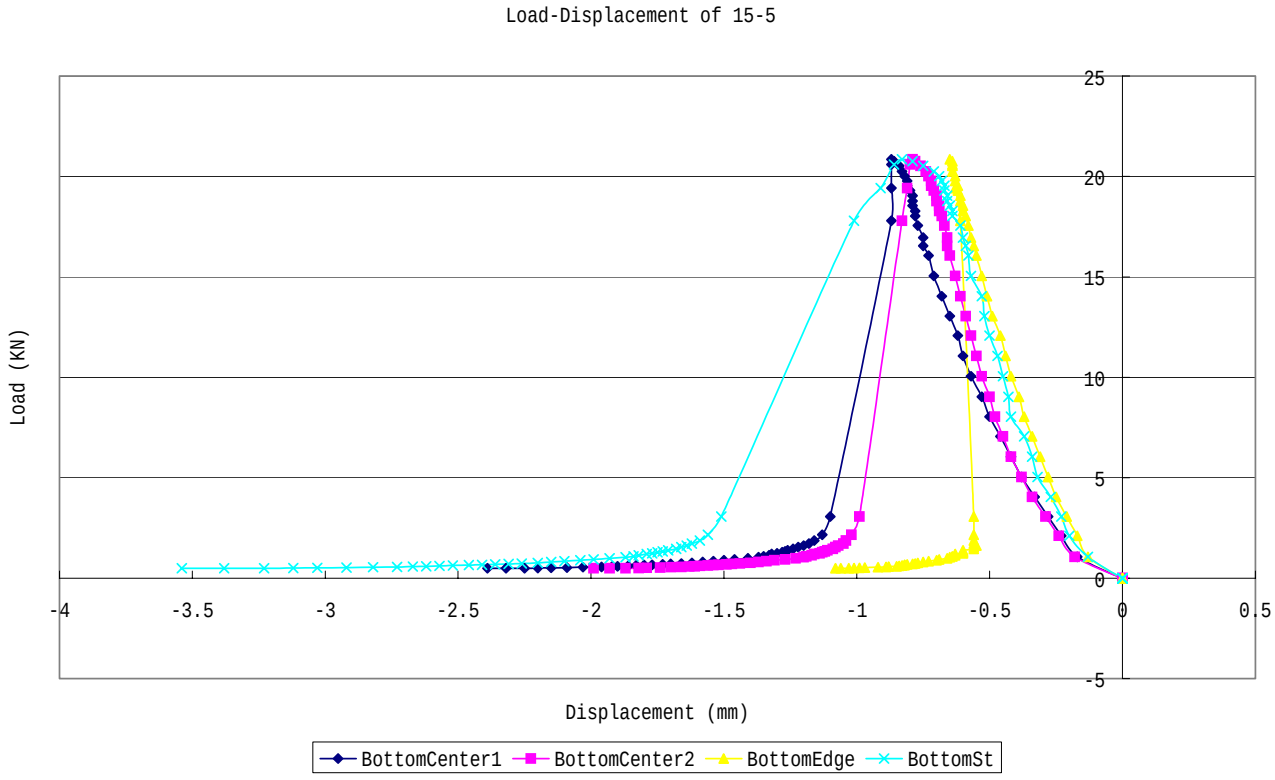

Figure 4.2 Original Data of Specimen 15-5

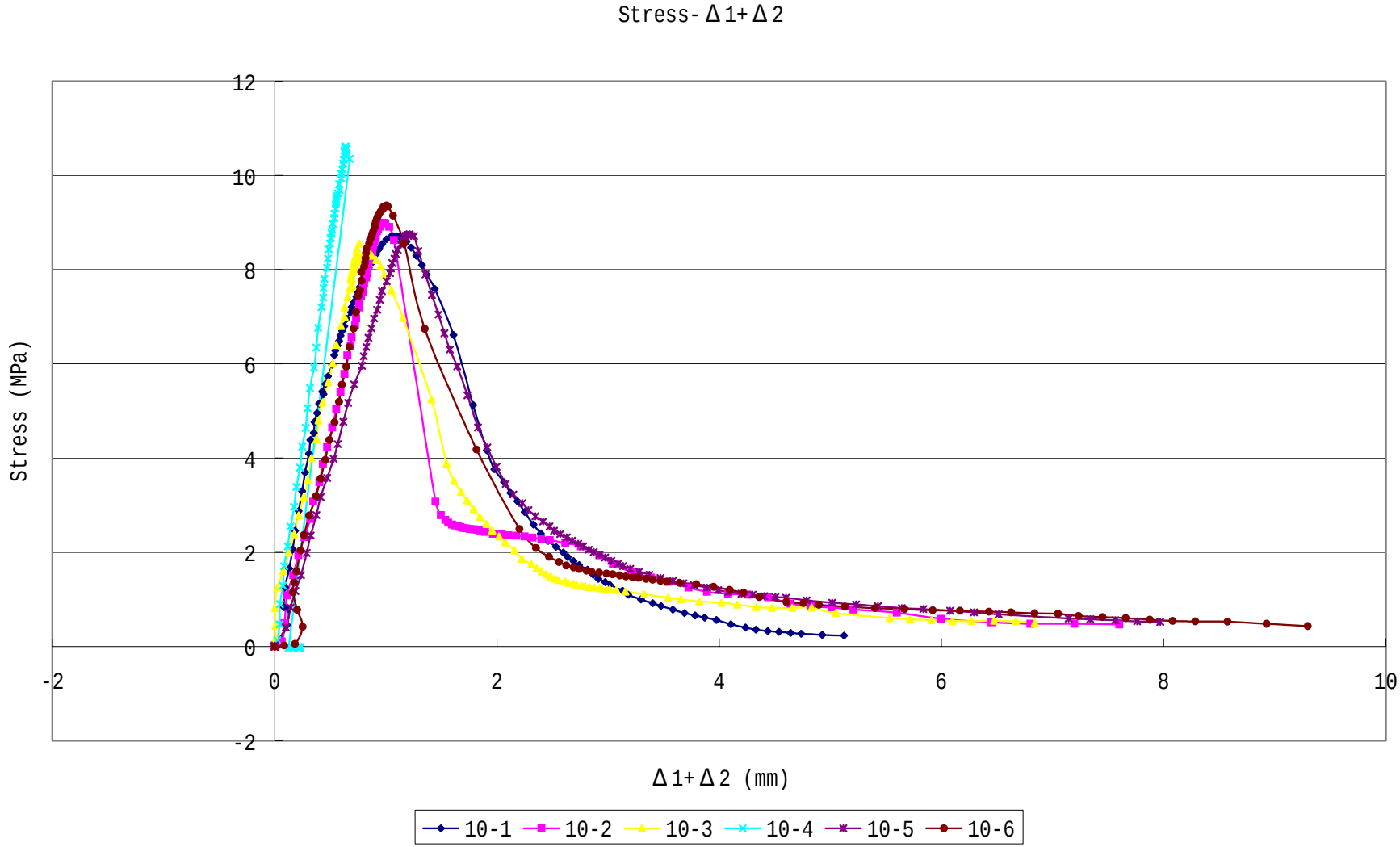

Figure 4.3 $\tau - \Delta_1 + \Delta_2$ relationship of Specimen Series 10

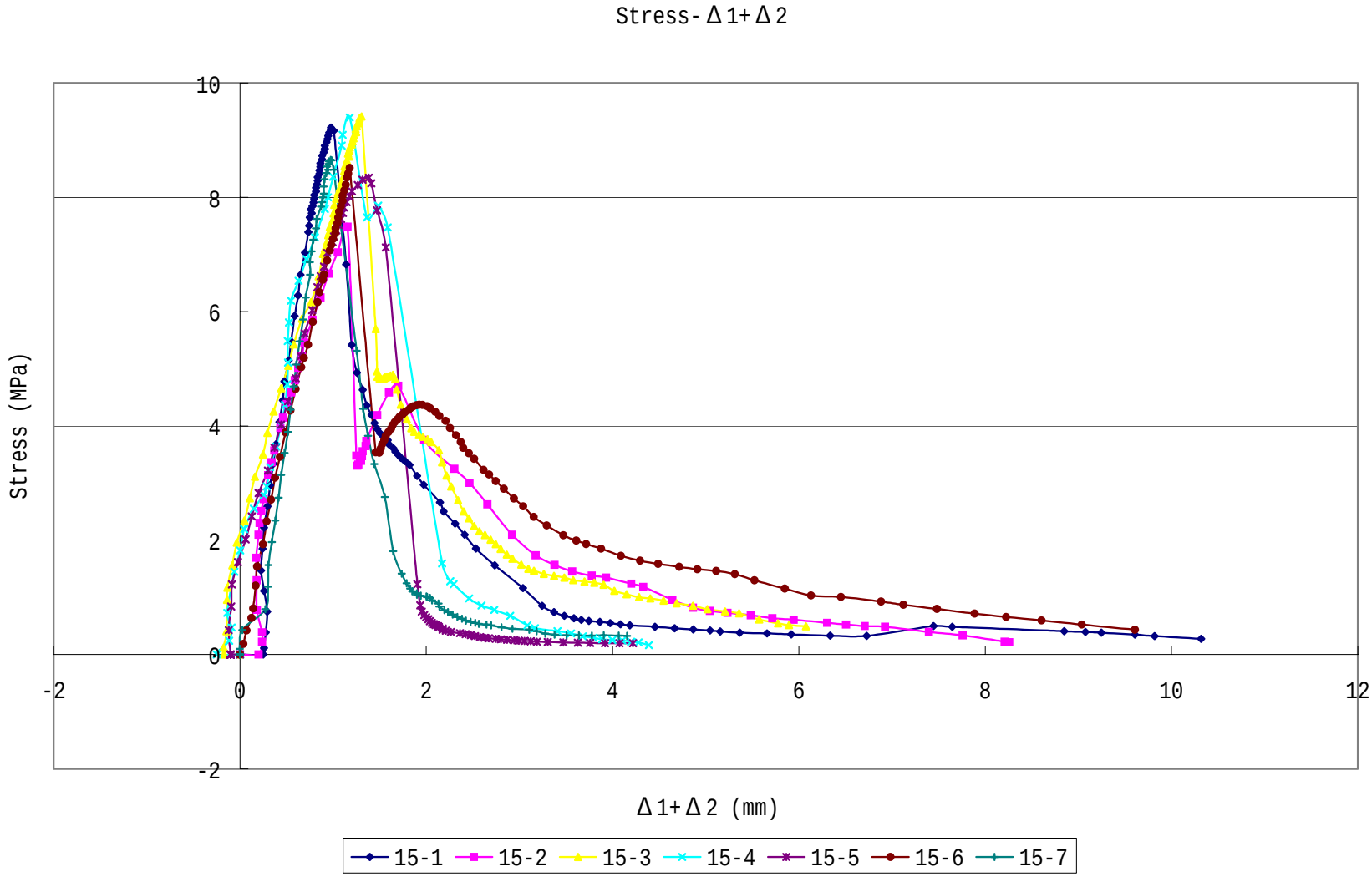

Figure 4.4 $\tau - \Delta_1 + \Delta_2$ relationship of Specimen Series 15

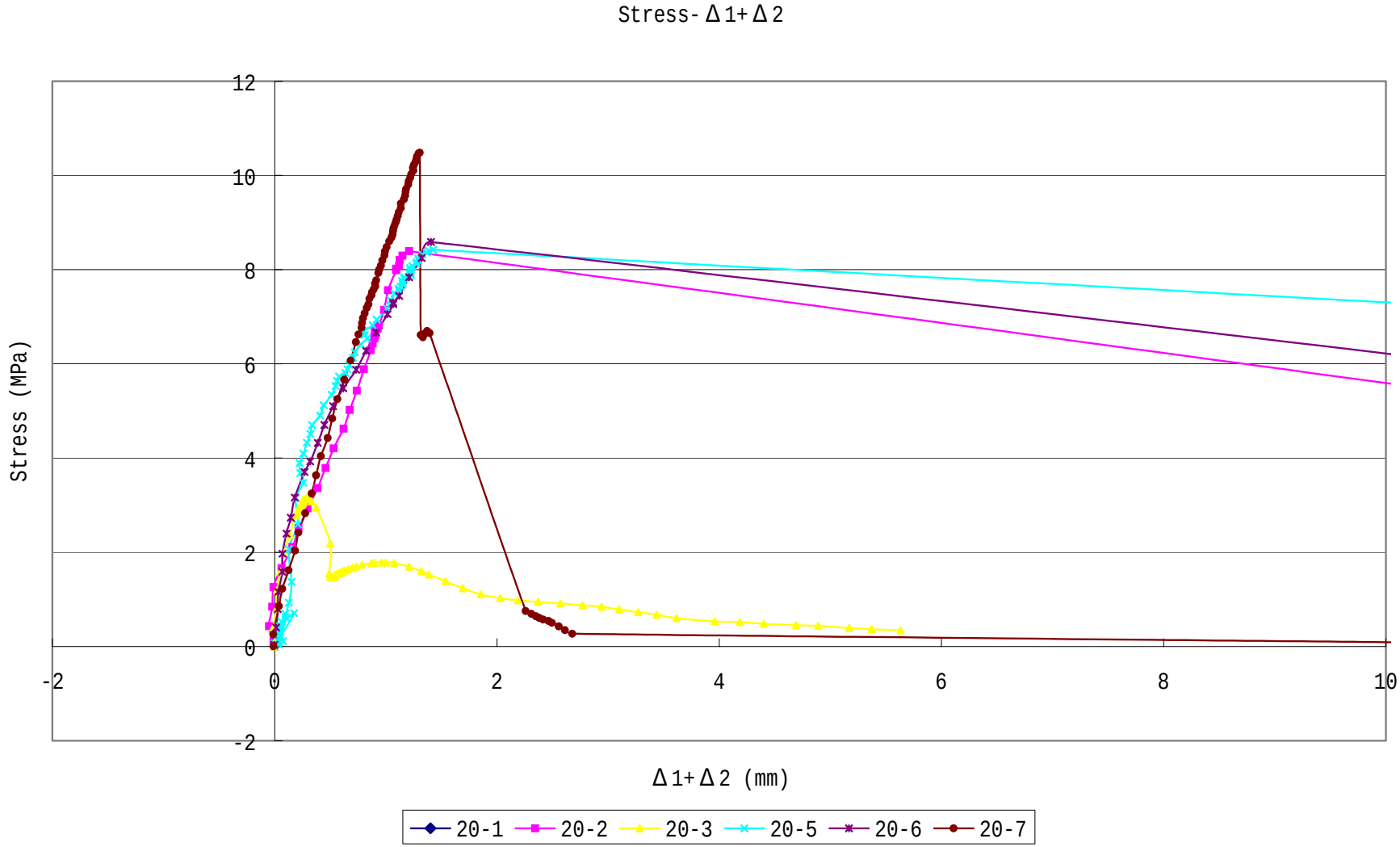

Figure 4.5 $\tau - \Delta_1 + \Delta_2$ relationship of Specimen Series 20

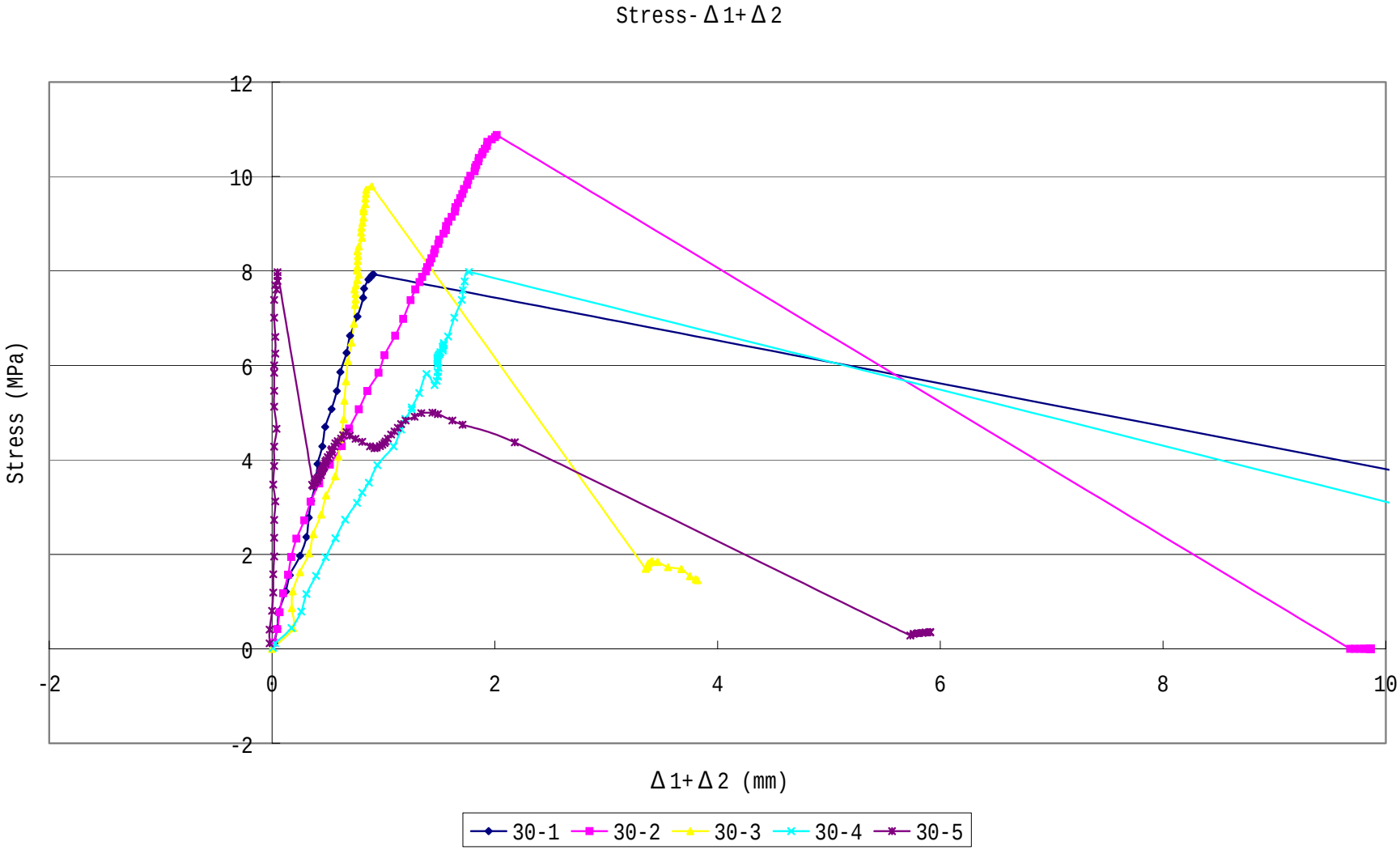

Figure 4.6 $\tau - \Delta_1 + \Delta_2$ relationship of Specimen Series 30

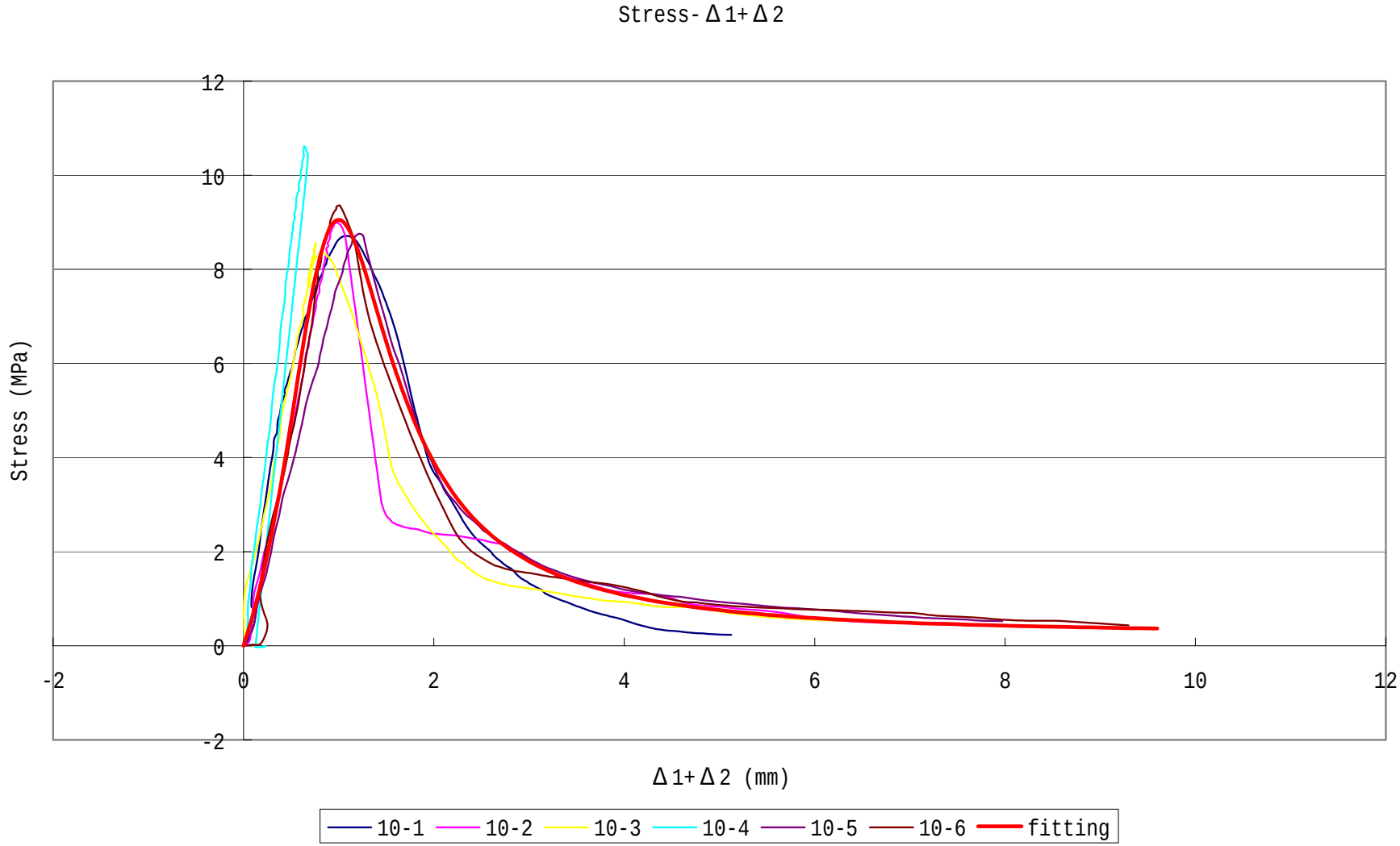

Figure 4.7 Curve Fitting for Specimen Series 10

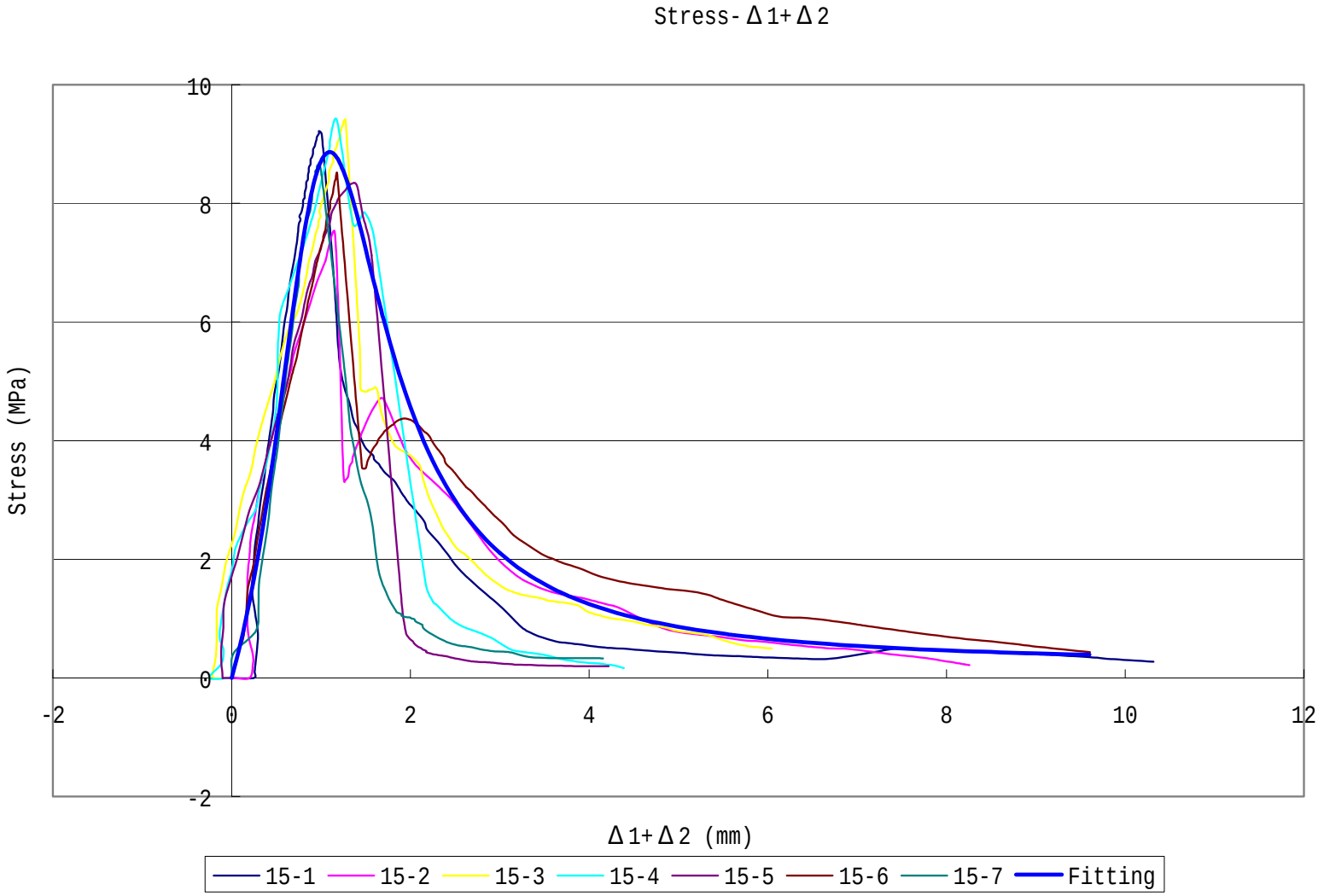

Figure 4.8 Curve Fitting for Specimen Series 15

§ 4.3 Influence of Height and Radius of Specimen

Figures 4.9 and *4.10* are the respective relationship between the bond strength and the height and radius of specimens. In our test, no obvious influences to the bond strength were found of the height and radius of specimens. We think this phenomenon can lead to the following conclusion:

(1) In our test, under the ultimate state, the bond stress of the specimen is evenly distributed. So the average bonding stress does not have obvious relationship with the height of the specimen. Hence, the test can be assumed to be under uniaxial loading.
(2) In our test, the minimum radius of the specimens is 10cm, which is 10 times the radius of the steel bar. So we consider that when the protect-layer size is 4.5 times lager than the dimension of the specimen, the influence of the protect-layer thickness to the bond strength is very small. Thus we can determine the size needed for Liu Yu's element when it is used in the finite element analysis.

§ 4.4 $\tau - \Delta$ Relationship at Peak Load Point

Figure 4.11 shows the relationship of $\tau - \Delta$ at the peak load of the specimens. The slope of the line is the secant stiffness of $\tau - \Delta$ on the peak load point. From this Figure and *Figures 4.3,* and *4.4,* we can consider that in the upward phase of the curve, the specimens' stiffness of slip is relatively concentrated.

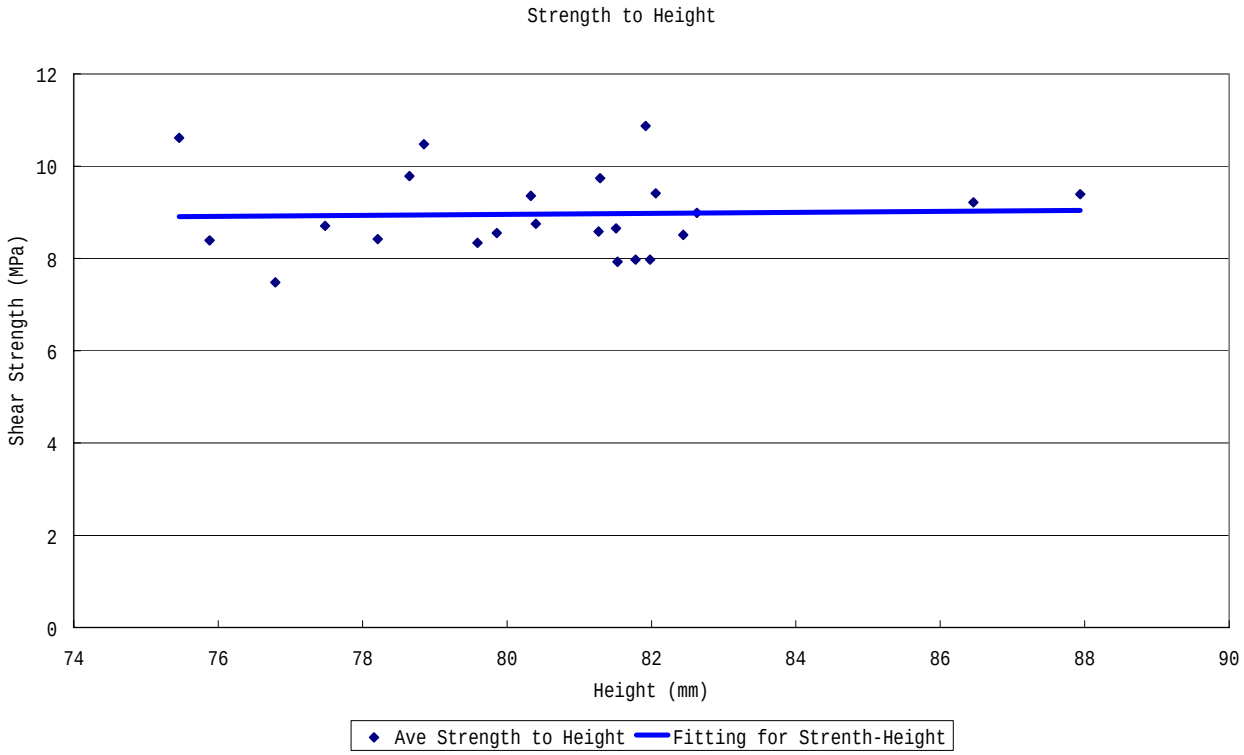

Figure 4.9 Relationship between Ultimate Strength and Height of Specimen

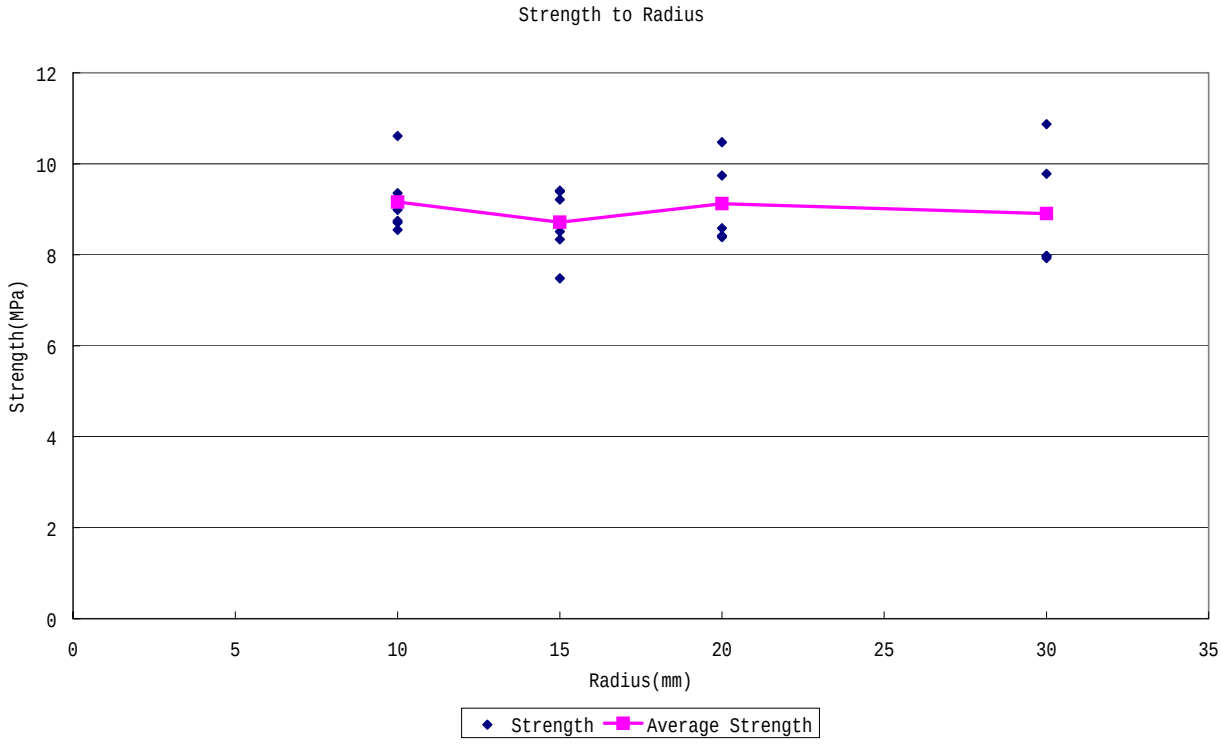

Figure 4.10 Relationship between Ultimate Strength and Radius of Specimen

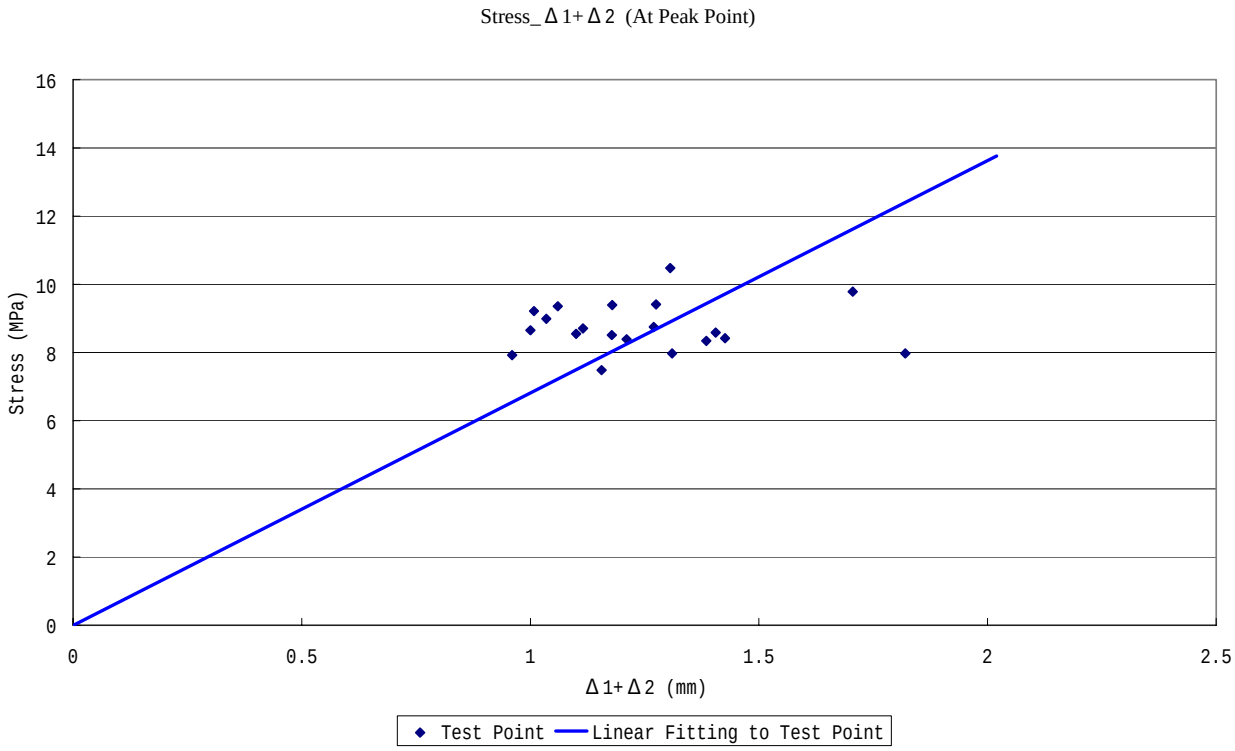

Figure 4.11 The $\tau - \Delta$ Relationship at Peak Load Point

§ 4.5 Shear Stress Distribution of Steel Bar and Deformation of Concrete

From the relationship between the bond strength and the height of the specimens shown in Section 4.3, we can assume qualitatively that on the peak load point, the shear stress of the specimen is evenly distributed. Because in RCED model, the slip field is assumed to be linear, so quantitatively analyzing the bond stress distribution is necessary.

From Section 4.4, we know that around the peak load point, the secant stiffness of $\tau - \Delta$ can be treated as a constant. So we can assume that at this point,

$$\tau = k\Delta \qquad (4\text{-}2)$$

In the linear slip field assumption of RCED model, we can obtain that

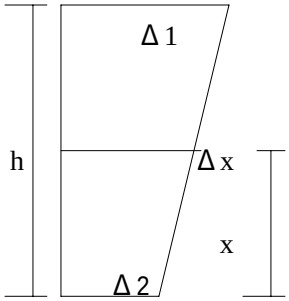

$$\Delta(x) = \Delta_2 + \frac{\Delta_1 - \Delta_2}{h} x \qquad (4\text{-}3)$$

in which h is the height of the specimen.

Since $\tau = k\Delta$, we can obtain that

$$\tau(x) = \tau_2 + \frac{\tau_1 - \tau_2}{h} x \qquad (4\text{-}4)$$

Let the axial force of the steel bar be *F*, hence

$$dF = \tau \pi D dx \qquad (4\text{-}5)$$

where D is the diameter of the steel bar,

The stress of the steel bar is $\sigma = \frac{F}{A} = \frac{F}{\pi D^2 / 4}$ (4-6)

The strain of the steel bar is $\varepsilon = \frac{\sigma}{E}$ (4-7)

Then the deformation of the steel bar in the whole specimen is

$$\Delta u = \int_0^h \varepsilon dx \qquad (4\text{-}8)$$

Δu is the relative displacement of the steel bar between the top and the bottom surface.

From Equations 4-5, 4-6, 4-7, 4-8, we can derive that

$$\Delta u = \int_0^h \frac{\int_0^h (\tau(x)\pi D + F_0) dx}{E \pi D^2 / 4} dx \qquad (4\text{-}9)$$

There is no force applied on the steel bar at the bottom end, $F_{x=0} = 0$

So we obtain

$$\Delta u = \int_0^h \frac{\int_0^h \tau(x) \pi D dx}{E \pi D^2 / 4} dx \qquad (4\text{-}10)$$

With Equations 4-10 and 4-4, we derive

$$\Delta u = \int_0^h \frac{\int_0^h (\tau_2 + \frac{\tau_1 - \tau_2}{h} x) \pi D dx}{E \pi D^2 / 4} dx \qquad (4\text{-}11)$$

Integrating Equation 4-11, we get

$$\Delta u = \frac{2h^2}{3ED}\tau_1 + \frac{4h^2}{3ED}\tau_2 \qquad (4\text{-}12)$$

We also know that $\bar{\tau} = \frac{\tau_1 + \tau_2}{2}$ (4-13)

where $\bar{\tau}$ is the average bond stress,

so finally

$$\tau_1 = 4\bar{\tau} - \frac{3\Delta uED}{2h^2} \qquad (4\text{-}14)$$

$$\tau_2 = \frac{3\Delta uED}{2h^2} - 2\bar{\tau} \qquad (4\text{-}15)$$

Let E=200GPa, D=10mm, and substitute Δu, h that we obtained from the test into Equations 4-14 and 4-15, we can derive τ_2 / τ_1 as shown in *Figure 4.12*. The average τ_2 / τ_1 is 0.813. So we can say that at this point, the bond stress is approximately evenly distributed, and linear assumption of RCED model is rational in this respect.

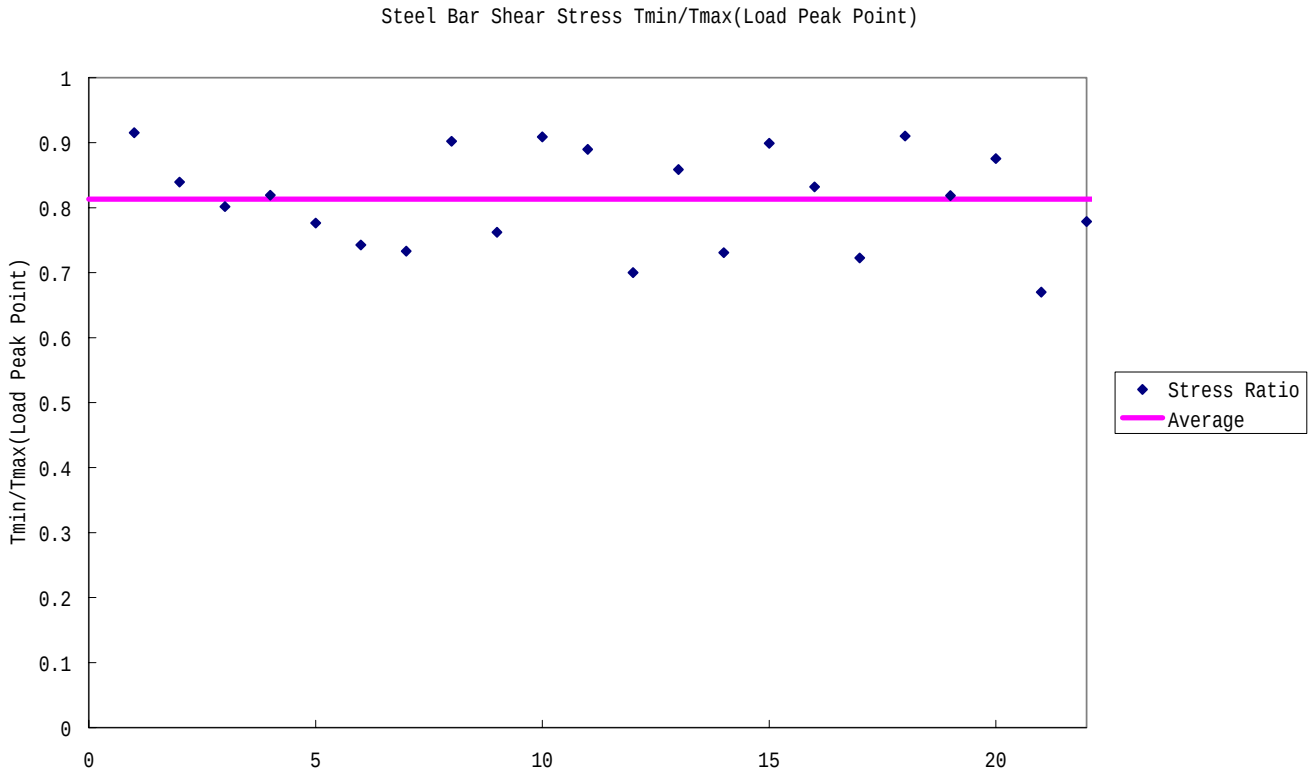

Figure 4.12 Bonding Stress Distribution on Peak Load Point

In the test, we also obtained the deformation of the top surface of the concrete which is shown in *Figures 4.13* and *4.14*. The load applied on the concrete is much more complex than the steel bar, so we will discuss it in Chapter 4. Numerical Computation. From the numerical result, it also proves that our linear assumption is reasonable.

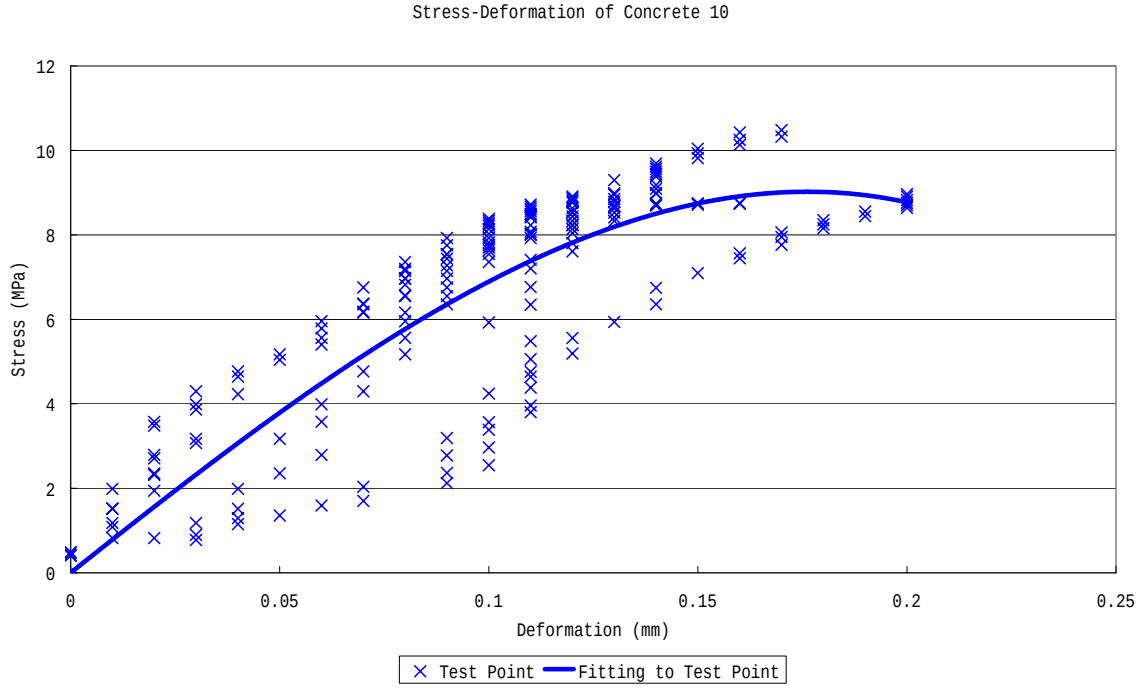

Figure 3.13 Deformation of concrete Specimen Series 10

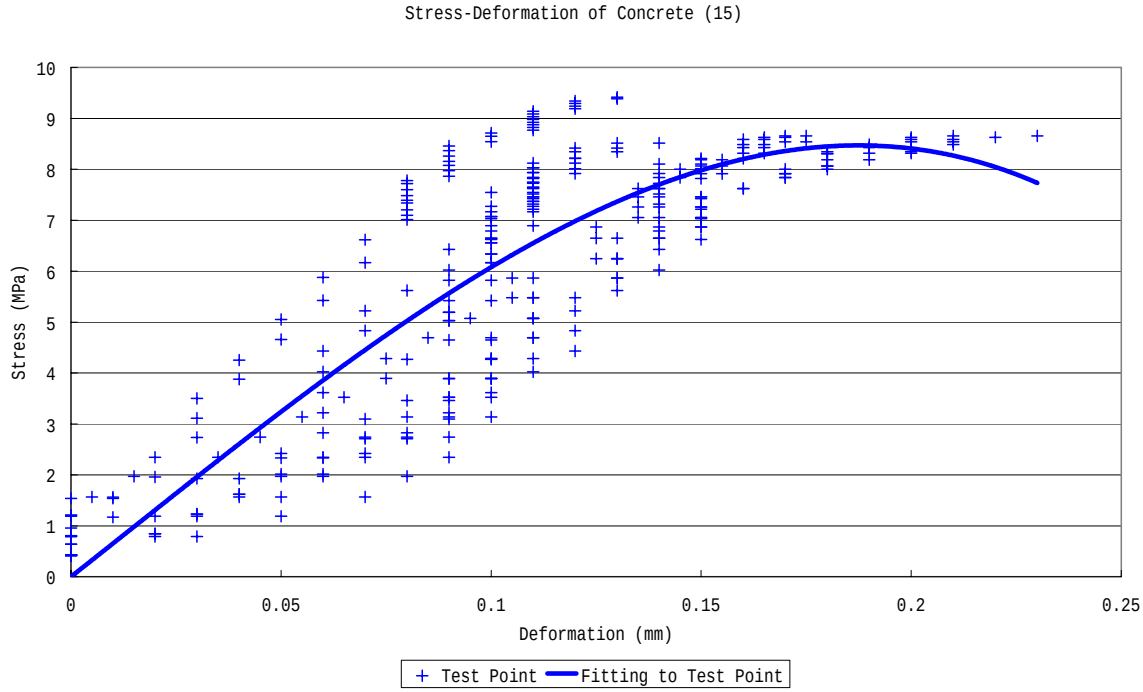

Figure 3.14 Deformation of concrete, Specimen Series 15

§ 4.6 Slip Damage Zone

We used UPV to determine the elastic module of concrete before and after the test. No obvious change is spotted. The cracks caused by slip are very small, and they all gathered around the bonding zone. So we consider that the local damage zone caused by the bond slip to be very small, since the detective device of the UPV is unable to determine the influence of the slip. Thus, the assumed local damage zone and the parameters α_1, α_2 will be derived from numerical computation.

Chapter 4 Numerical Computation

§ 4.1 Objectives of Numerical Computation

1. Through the test, we obtain the bond-slip constitutive relationship. As discussed in Chapter 2, we let the specimens in our test as thin as possible, because we hope the result obtained from the test can be used in the numerical analysis directly. In the following numerical computation, we put the bond-slip constitutive relationship obtained from the test into the bond elements. If the numerical result is consistent with the test result, we can say that it is reasonable to use the empirical constitutive relationship directly in the numerical analysis.

2. Because of the limitation of measuring method, some data are very difficult to measure, such as the slip field in the specimen. However, in Liu Yu's reinforcement element model, the slip field is assumed to be linear, and we want to know whether the assumption is suitable or not. If the numerical result is consistent with the test result, we can consider that the numerical computation reflects the real condition correctly. So we can use the slip field obtained from the numerical analysis to verify Liu's assumption.

§ 4.2 Material Constitutive Relationship

1. Concrete

The constitutive relationship we use in the finite element analysis is Hogenestad model, which can be expressed as

$$\sigma = \sigma_0 \left[2\varepsilon / \varepsilon_0 - \left(\varepsilon / \varepsilon_0 \right)^2 \right] \qquad 0 \le \varepsilon \le \varepsilon_0$$

$$\sigma = \sigma_0 \left[1 - 0.15 \frac{\varepsilon - \varepsilon_0}{\varepsilon_u - \varepsilon_0} \right] \qquad \varepsilon_0 \le \varepsilon \le \varepsilon_u$$

in which σ_0 is the maximum principle stress, ε_0 is the strain when the maximum principle stress is equal to σ_0, ε_u is the ultimate strain.

2. Steel

In our test, the maximum stress of the steel bar is about 350Mpa, which is smaller than the yield stress of the steel bar, σ_y=500 MPa. So the steel is treated as linear elastic material and its elastic module is used.

3. Bonding Zone

The constitutive relationship of the bond between concrete and rebar is as follows:

$$\tau = \frac{0.7260\tau_{\max}(\frac{\xi}{\xi_0}) + 0.061(\frac{\xi}{\xi_0})^{3.2}}{1 - 0.916(\frac{\xi}{\xi_0}) + 0.642(\frac{\xi}{\xi_0})^{2.87}}$$

which is obtained from the test.

4. Glue and PVC Pipe

The force acting on the glue and PVC pipe is several MPa only. It is very small. So they are all treated as linear elastic materials.

§ 4.3 Finite Element Analysis Software

We use MARC k 7.3.2 to do the linear analysis and SAP 91 to do the non-linear analysis.

§ 4.4 The Element Type and Mesh

The concrete, steel bar, glue and PVC pipe is meshed with 3D 20 nodes isoparametric element and the bonding zone is meshed with spring element. The mesh is shown as *Figure 4.1,* and *4.2*.

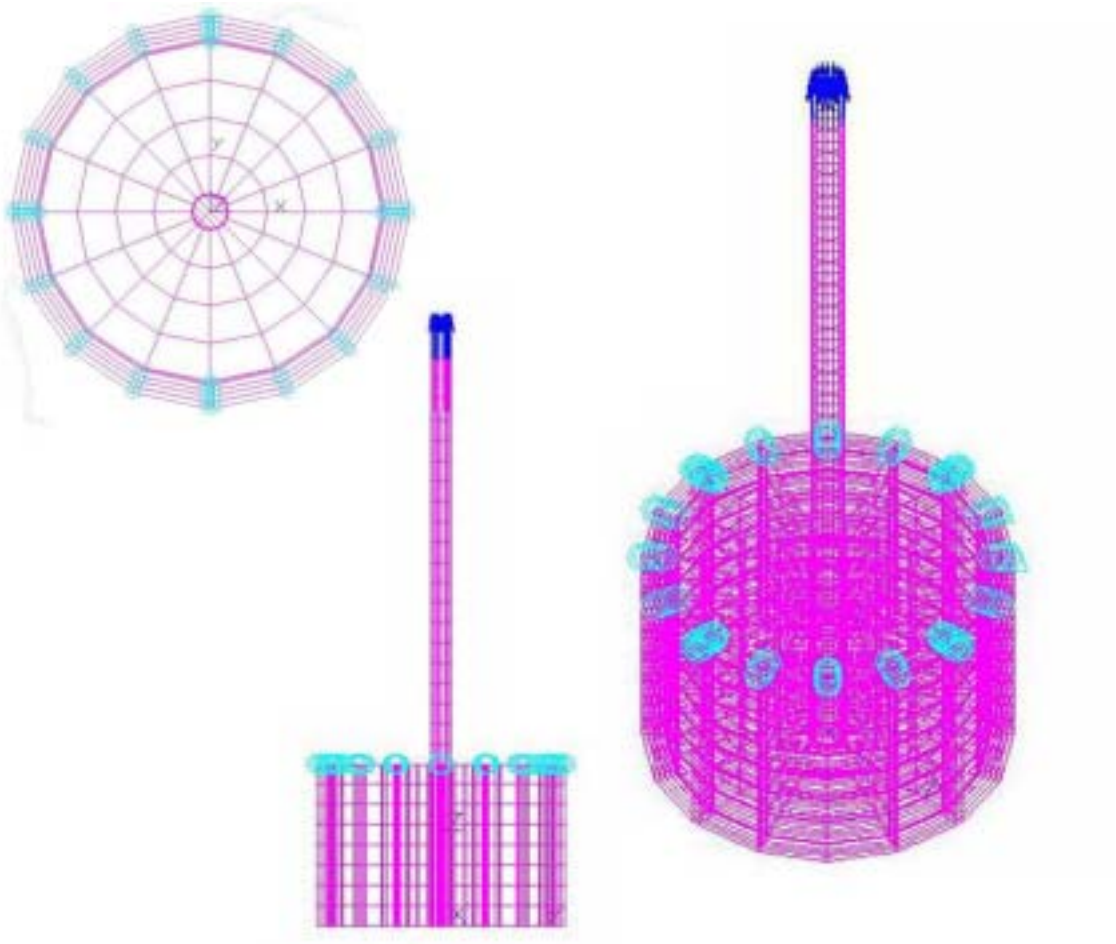

Figure 4.1 Mesh of Specimen 10

§ 4.5 Numerical Results

The displacement of steel bar and concrete on the top and bottom surface is shown in Table 4.1 for Group 10 and 4.2 for Group 15, respectively. Along the bar, on the peak load point, the displacement of concrete and steel bar and the bonding stress is shown in Table 4.3 and 4.4. The displacement figure is shown as *Figure 4.3, 4.4.*

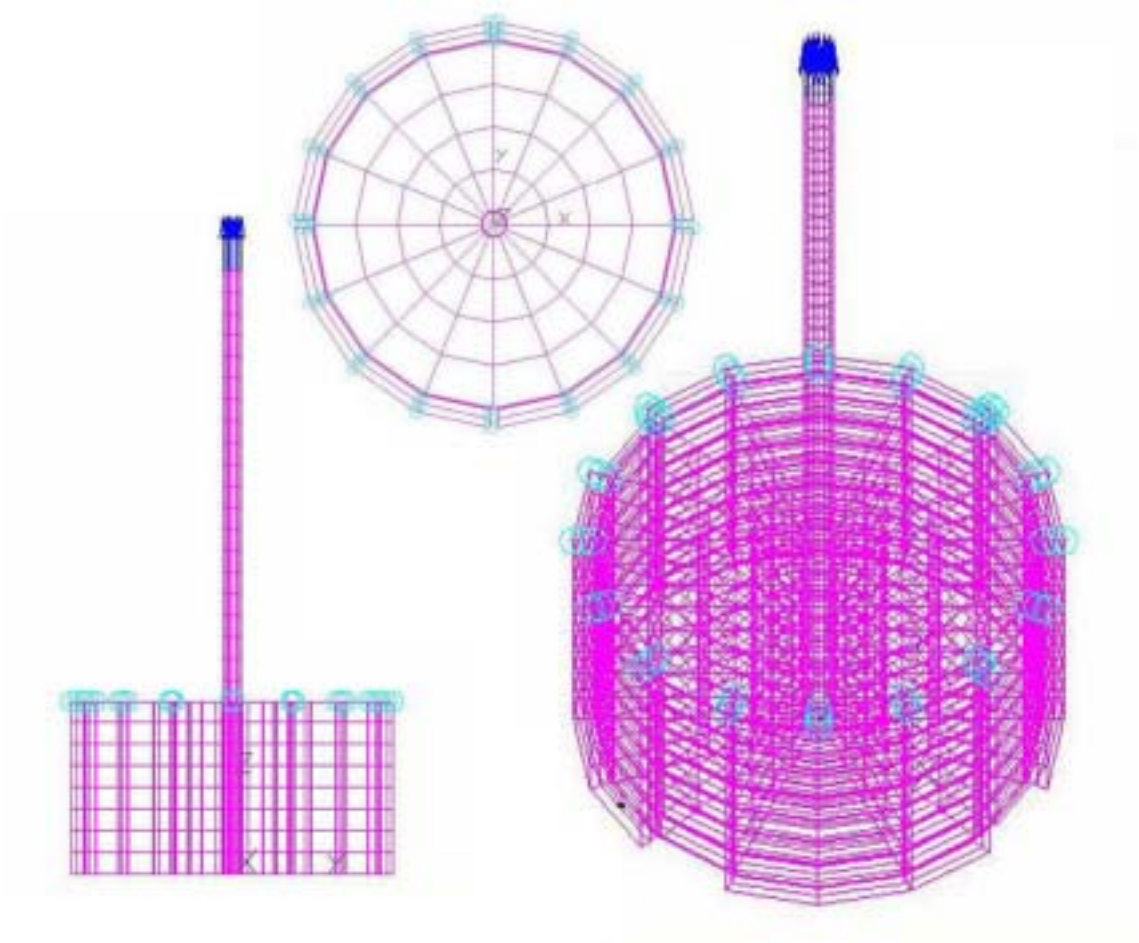

Figure 4.2 Mesh of Specimen 15

Table 4.1 Group 10 Displacement of Concrete and Steel Bar on Top and Bottom Surface

Load (KN)	Average Shear Stress (MPa)	Displacement of Steel Bar on Top Surface (mm)	Displacement of Steel Bar on Bottom Surface (mm)	Displacement of Concrete Top Surface (mm)	Displacement of Concrete Bottom Surface (mm)
0	0	0	0	0	0
5.655	2.25	0.1891	0.1101	0.03237	0.02481
11.31	4.5	0.3858	0.2274	0.06772	0.05259
16.965	6.75	0.6004	0.3616	0.1077	0.09004
22.62	9	0.8769	0.5550	0.1575	0.1256

Table 4.2 Group 15 Displacement of Concrete and Steel Bar on Top and Bottom Surface

Load (KN)	Average Shear Stress (MPa)	Displacement of Steel Bar on Top Surface (mm)	Displacement of Steel Bar on Bottom Surface (mm)	Displacement of Concrete Top Surface (mm)	Displacement of Concrete Bottom Surface (mm)
0	0	0	0	0	0
5.655	2.25	0.1976	0.1187	0.03965	0.03281
11.31	4.5	0.4038	0.2456	0.08311	0.06901
16.965	6.75	0.6293	0.3908	0.1326	0.1108
22.62	9	0.9203	0.5986	0.1952	0.1660

Table 4.3 Group 10 Displacement and Bonding Stress along Steel Bar

Distance to Top Surface (cm)	Displacement of Steel Bar (mm)	Displacement of Concrete (mm)	Bonding Stress (MPa)
0	0.8769	0.1575	7.996467
1	0.7958	0.1564	8.762194
2	0.7289	0.1424	9.026656
3	0.6737	0.1325	9.016539
4	0.6301	0.1261	8.813545
5	0.5970	0.1229	8.51776
6	0.5739	0.1232	8.207353
7	0.5602	0.1276	7.923785
8	0.5550	0.1256	7.870022

Table 4.4 Group 15 Displacement and Bonding Stress along the Steel Bar

Distance to Top Surface (cm)	Displacement of Steel Bar (mm)	Displacement of Concrete (mm)	Bonding Stress (MPa)
0	9.203	1.952	7.932148
1	8.393	1.968	8.739265
2	7.725	1.869	9.028785
3	7.174	1.782	9.010252
4	6.739	1.721	8.795787
5	6.408	1.689	8.491437
6	6.177	1.686	8.18375
7	6.04	1.704	7.940371
8	5.986	1.66	7.923785

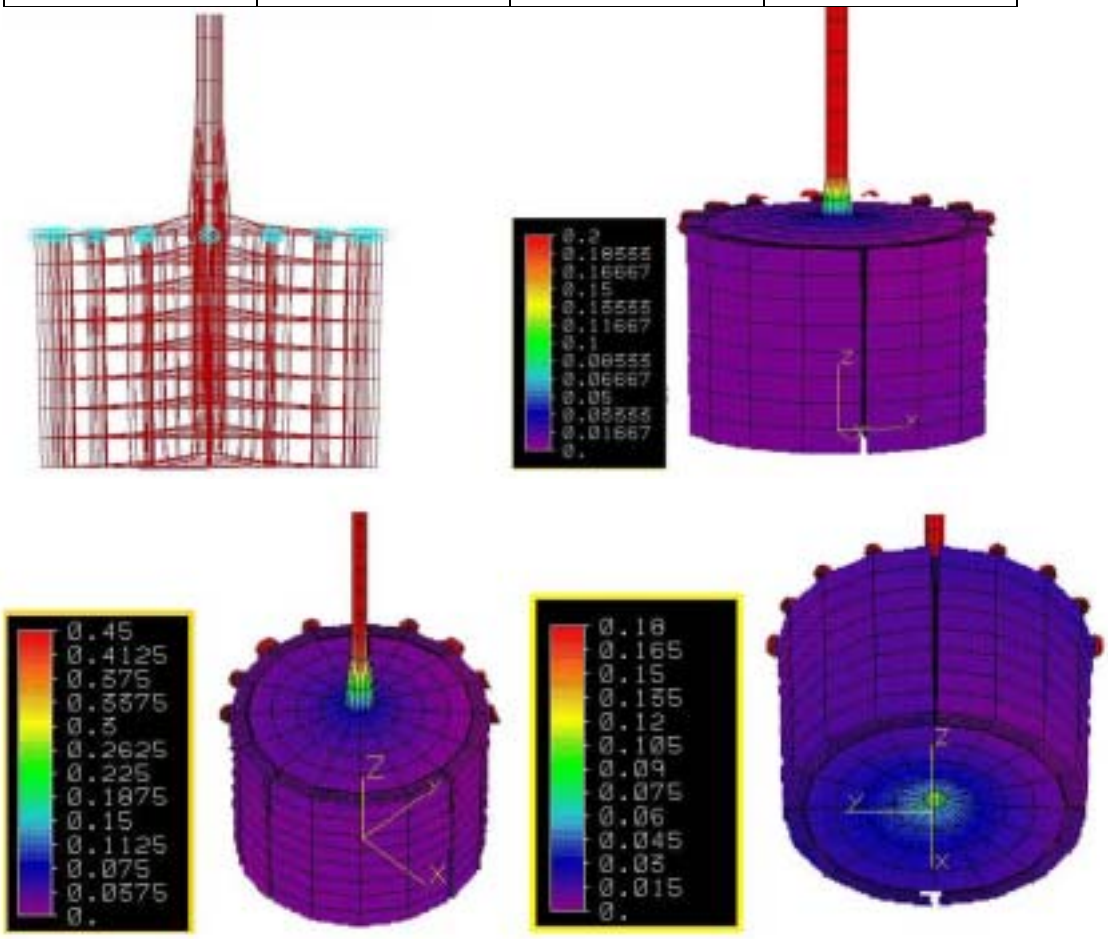

Figure 4.3 Displacement of Group 10

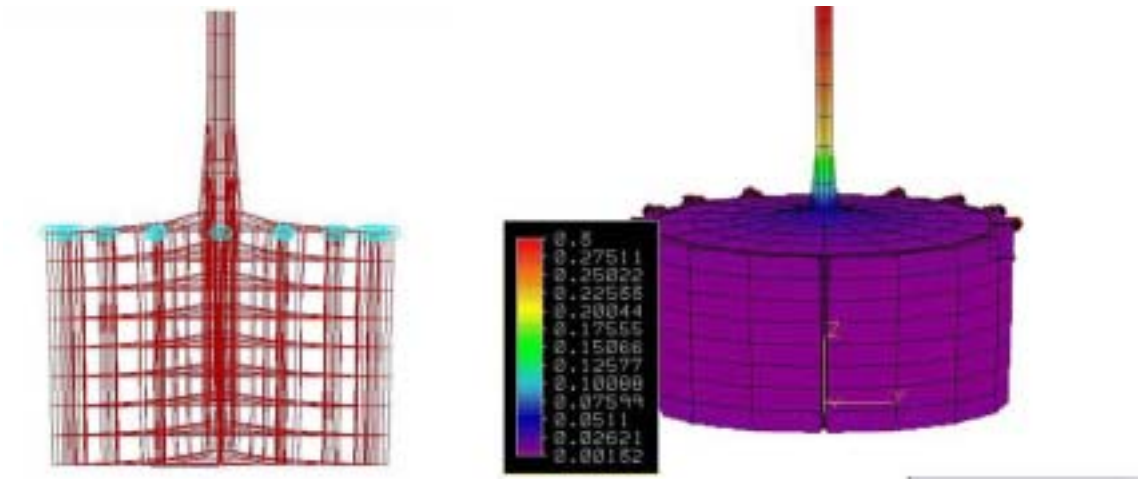

Figure 4.4 Displacement of Group 10

§ 4.6 Compare to the Results

The curves of relationship of $\tau - \Delta_1 + \Delta_2$, which are obtained from test and numerical calculation, are shown in *Figure 4.5*, where τ is the average shear stress. $\Delta_1 + \Delta_2$ is the sum of relative displacement between the steel bar and concrete on top and bottom surfaces.

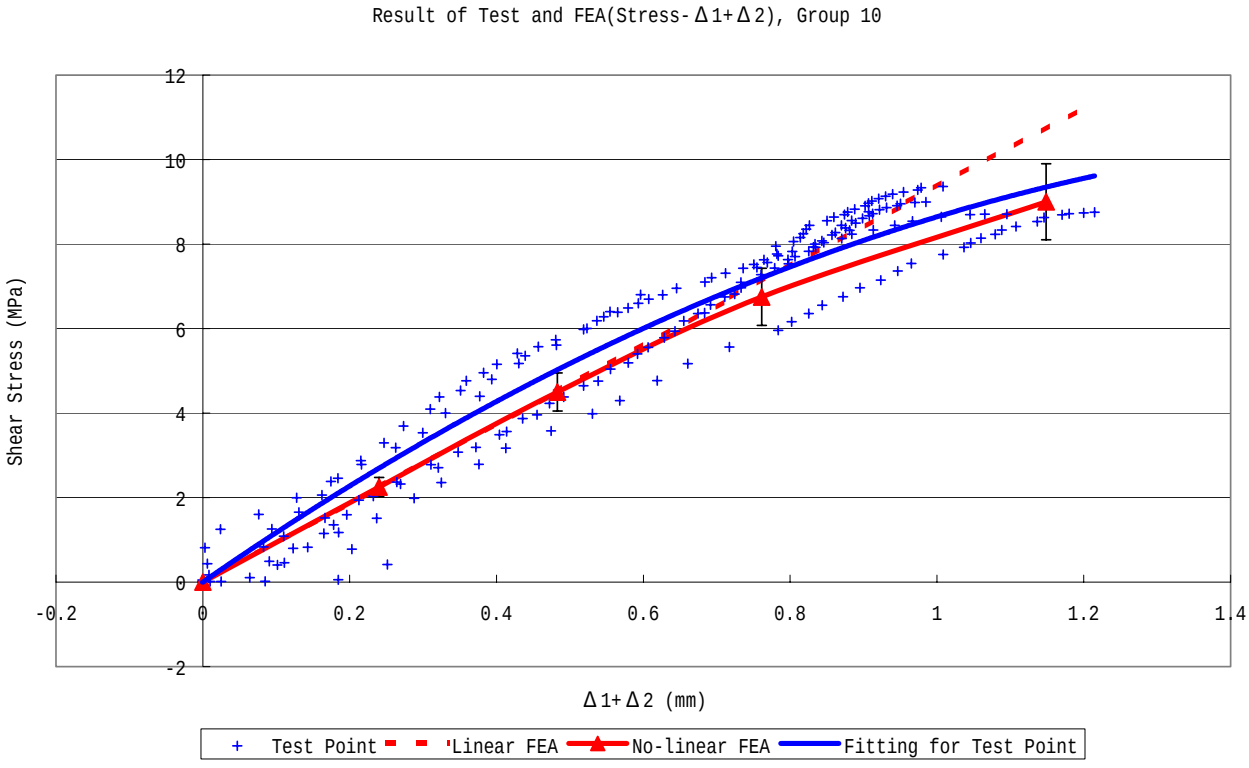

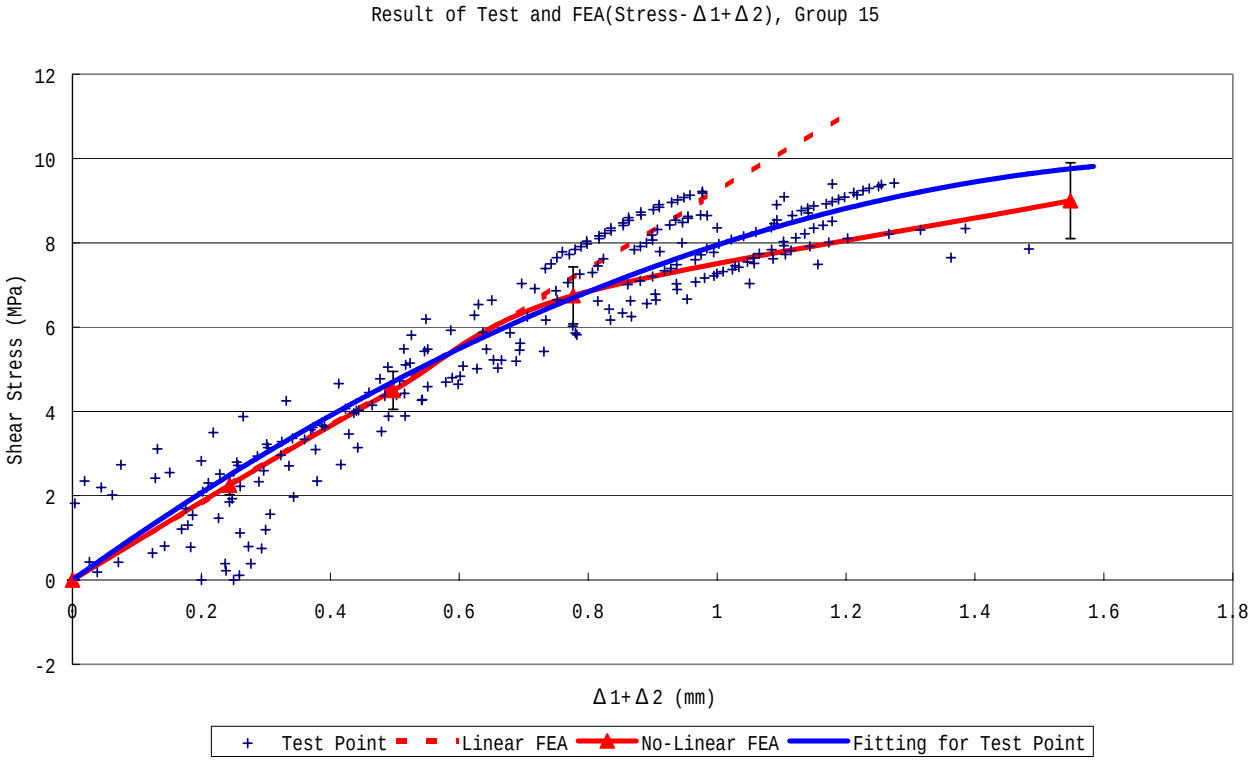

Figure 4.5 The Test and Computation Result of $\tau - \Delta_1 + \Delta_2$

The experimental and numerical results of $\tau - \Delta$ relationship are shown in *Figure 4.6*. Here τ is also the average shear stress and Δ is relative displacement of concrete between the top surface center and top surface edge.

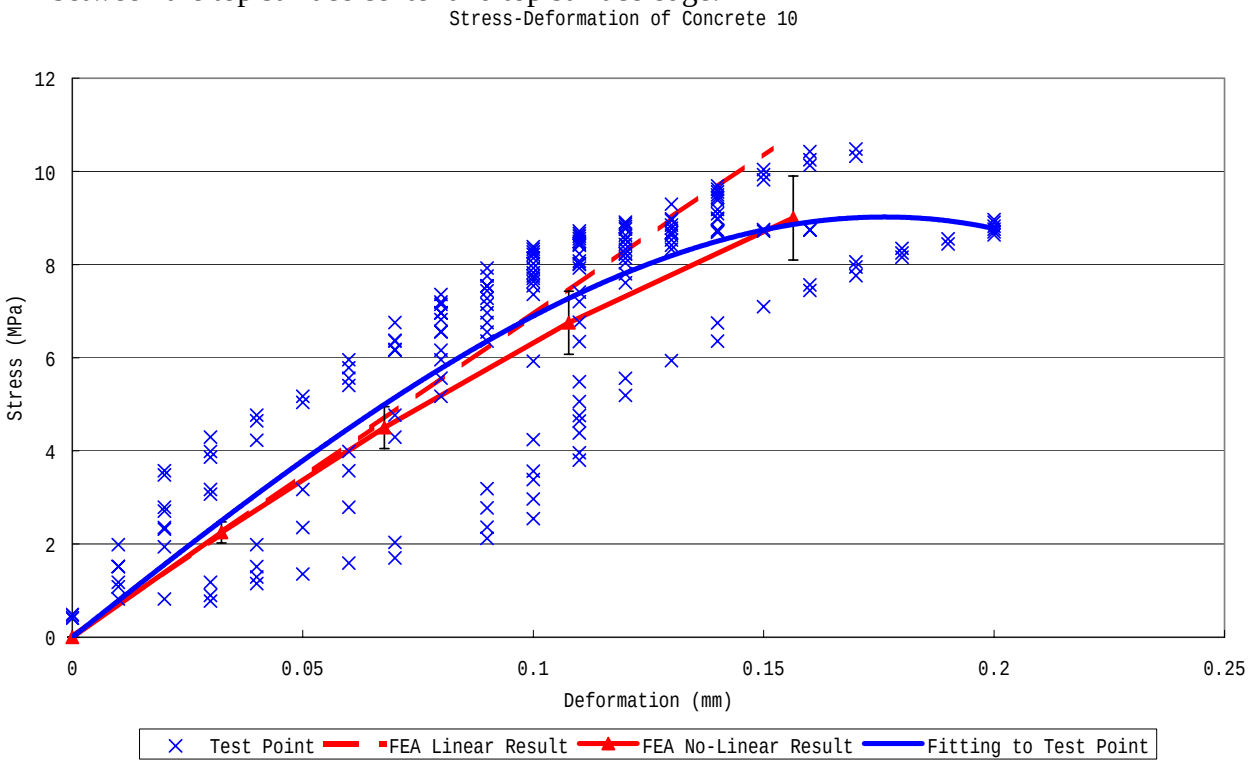

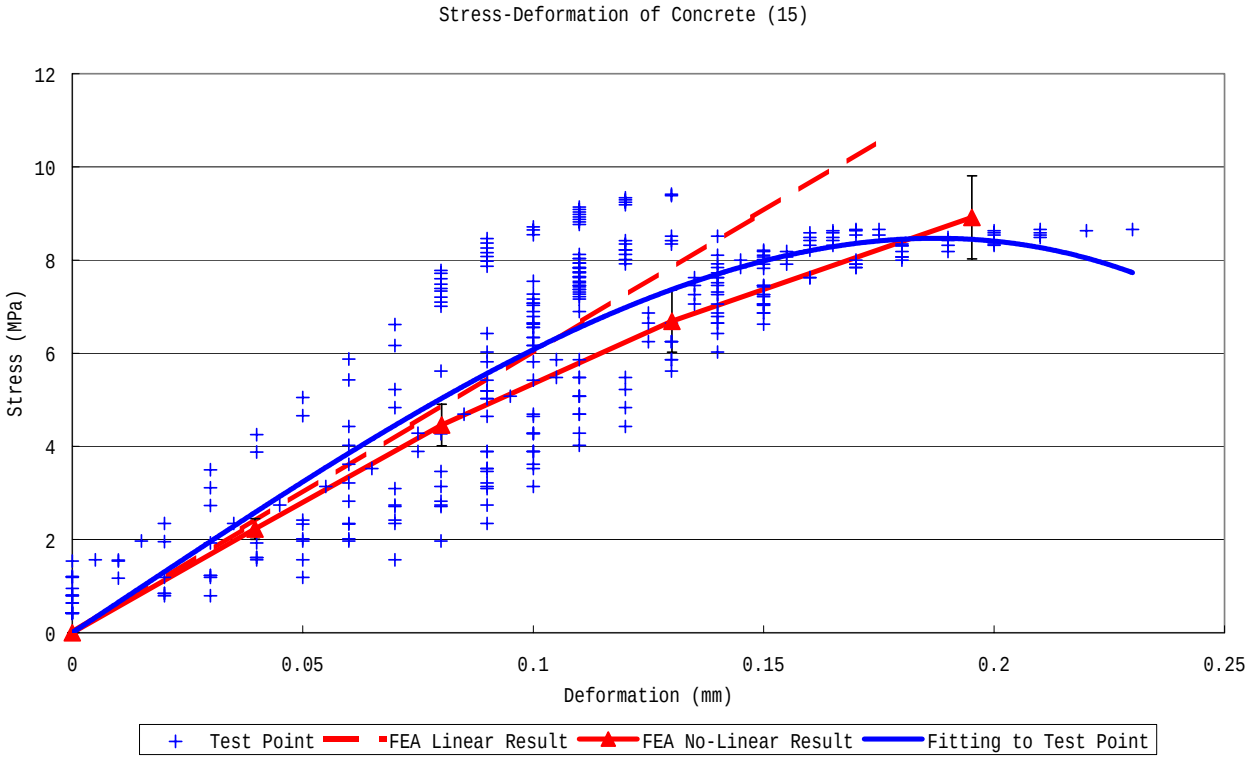

Figure 4.6 The Test and Computation Result of $\tau - \Delta$

From the above two figures, we can see that the error between the experimental and numerical results is less than 10%. So we consider that the two results are consistent. We use bond-slip constitutive relationship obtained from the test directly in numerical analysis is rational.

In the bonding zone of specimen, the computed slip field is shown in *Figure 4.7*. Two conclusions can be obtained from this figure. First is that when the protect-layer is lager than 4.5 times of the re-bar's diameter, the influence of the protect-layer size to the slip field is very small. Second is that although the slip field is not precisely linear, yet it is reasonable to use linear distribution to approximate the real state, as the linear degree of the field is about 0.925,

On the peak load point, the shear stress distribution along the re-bar is shown in *Figure 4.8*. The stress distribution is very even. And if we let τ_2 / τ_1 to be 0.813, just as we discussed in §3.6, we can see that the linear assumption is quite close to the real state.

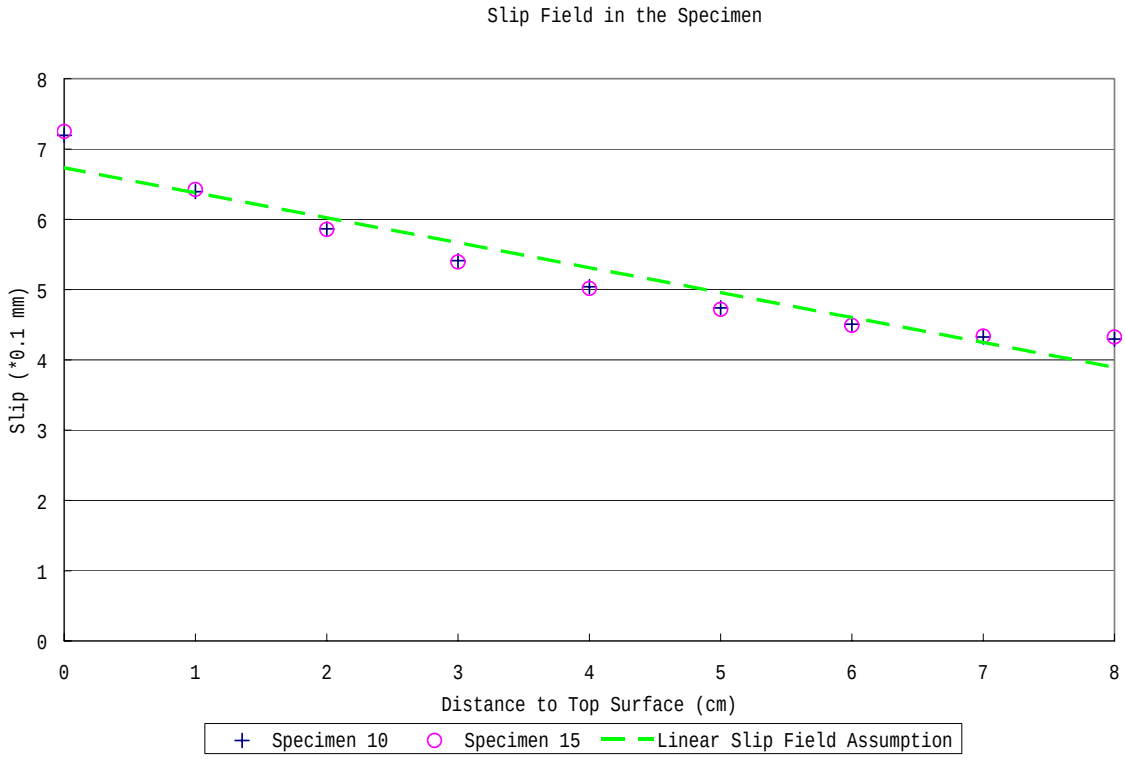

Figure 4.7 Slip Field in Specimen on Peak Load Point

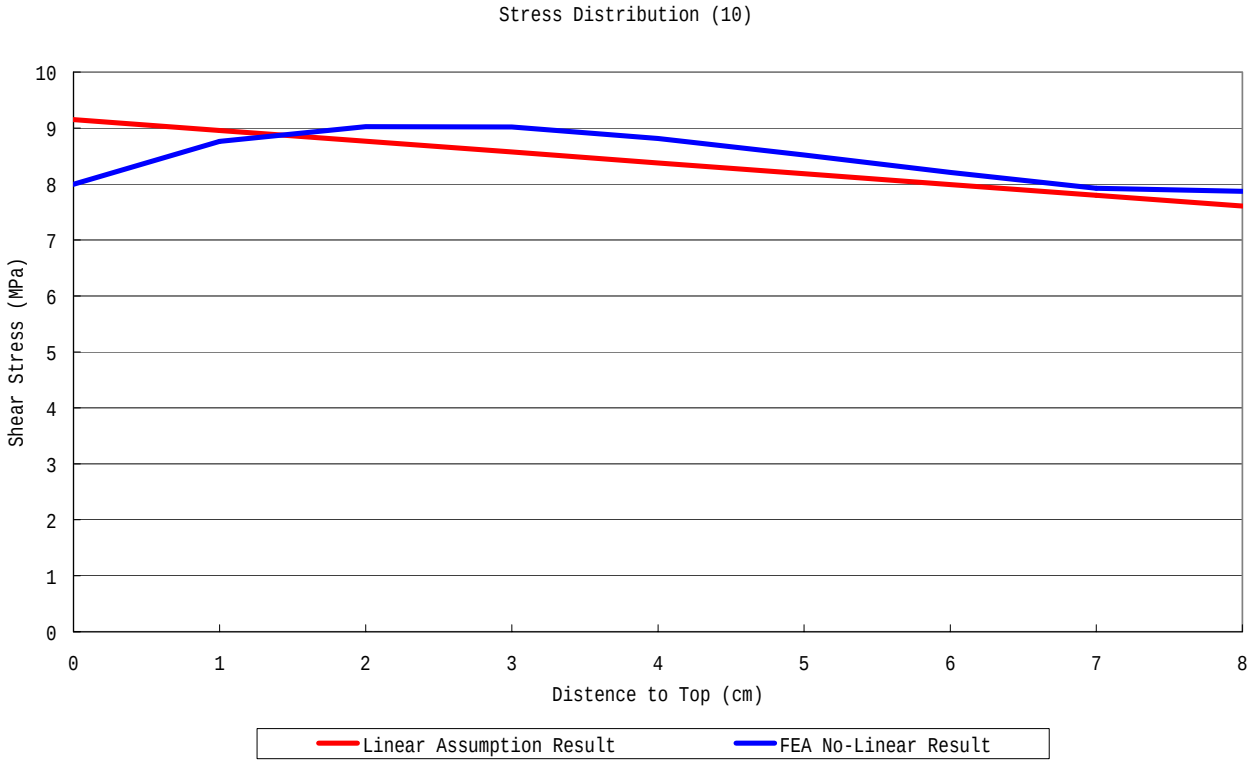

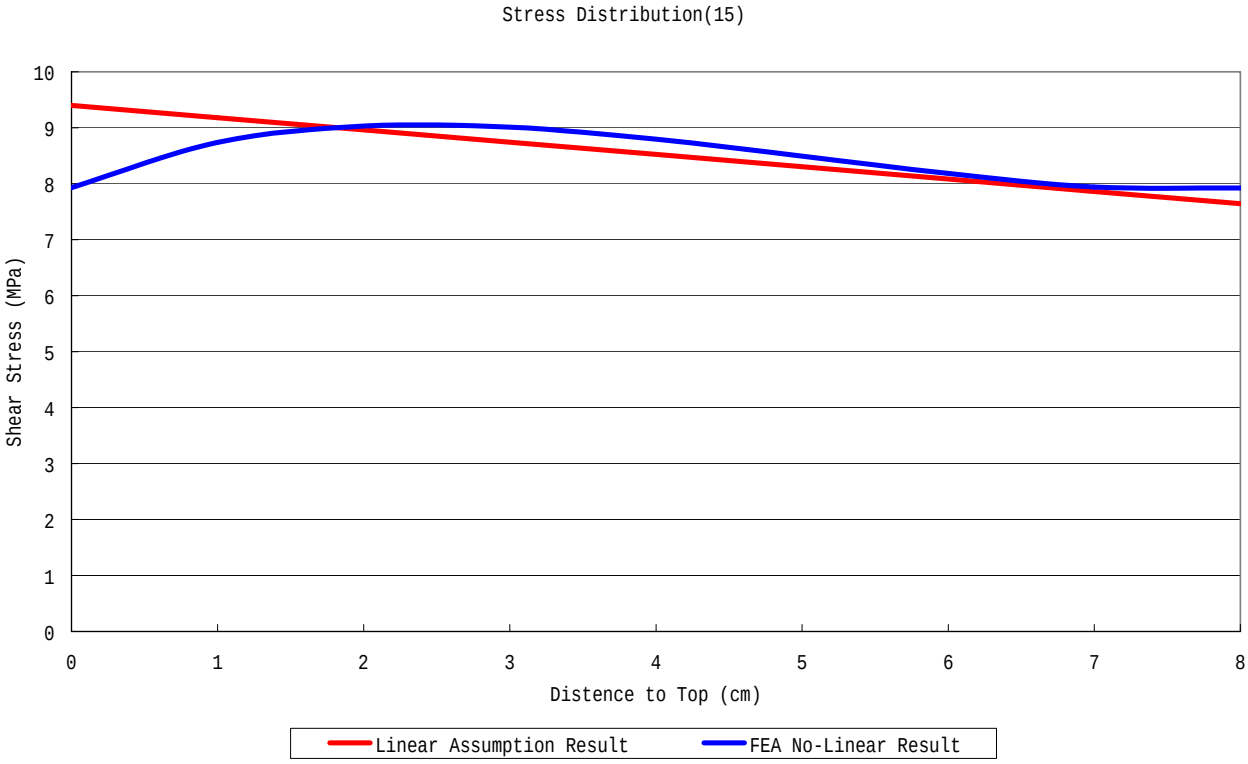

Figure 4.8 Stress Distribution in Specimen on Peak Load Point

Figure 4.9 shows the change of bond stress distribution with load. We can see when load approach to the peak point, bond zone near to the top surface damages first.

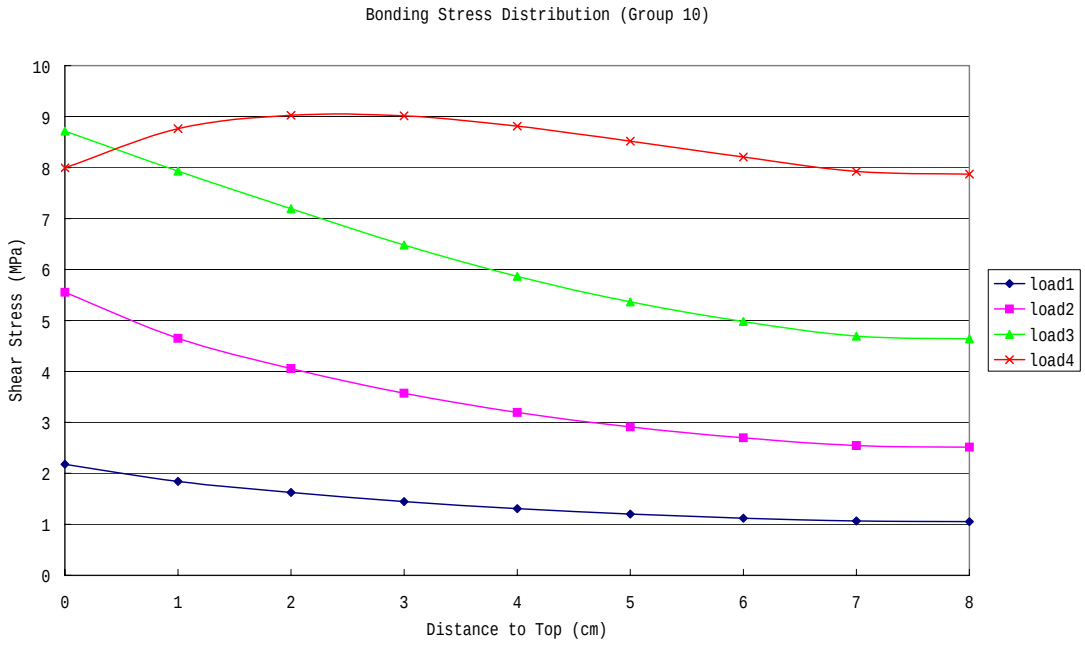

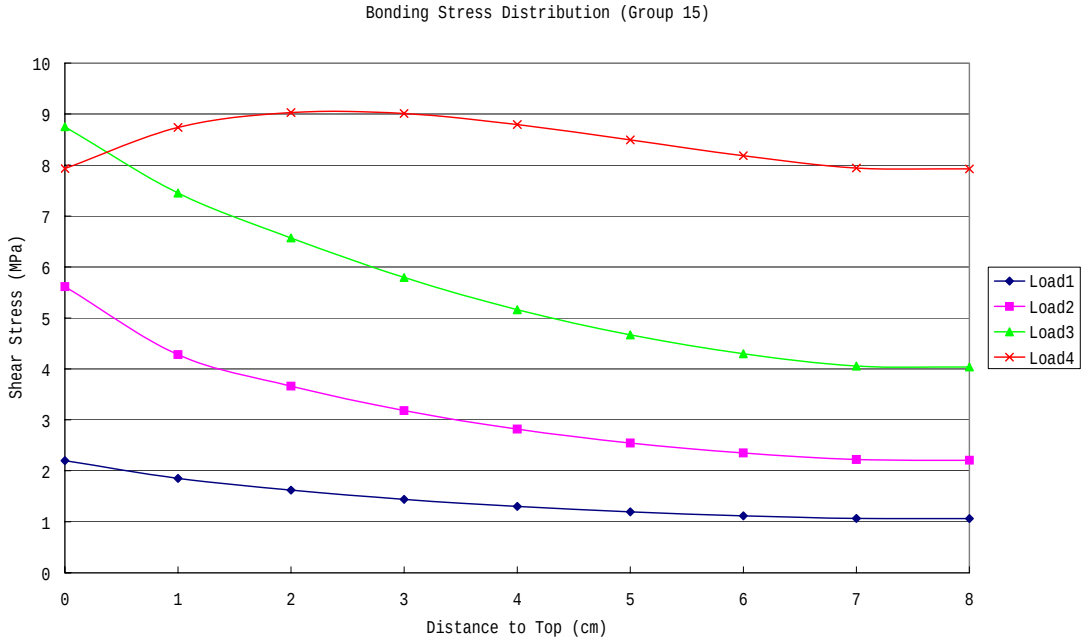

Figure 4.9 Change of Bonding Stress Distribution with Load.

Chapter 5 Conclusions

All structure tests serve for the following two purpose: one is for the application in real structures, the other is for the theoretical analysis. The former requires the test as close to the real structures as possible, so as to reflect the behavior of structure in real complex stress-state. However, the later hopes that the stress-state in the test is as simple as possible, so does the boundary conditions, so that the experimental test can simulate the ideal conditions in the theoretical analysis. Our test belongs to the later type. In our test, the concrete is under the pure shear stress condition along the re-bar direction. The influence of stresses in other directions is very small. We found from the test results and numerical calculation that: For the specimens tested, the linear degree of the slipping field is 0.925, the linear degree of the bonding stress is 0.941 and the shear stress ratio of the minimum value to the maximum one is 0.813. So we can see that the stress-state, deformation-shape and boundary condition are all very simple and clear. The test provides some useful data for the theoretical analysis in the future.

From the test results, the following conclusions can be made:

(1) Four groups of concrete specimens are tested and the experimental load-deformation relationships of 23 specimens are obtained. From the test data, the full curves of the relationship of $\tau - \Delta_1 + \Delta_2$ are calculated. The curves are fitted and an empirical formula is proposed.

(2) From the test results, it is spotted that the local damage zone in the concrete caused by the bond-slip is very small. It is limited to the zone near the interface between the concrete and the steel bar. The size of the specimen has little influence on the local damage zone.

(3) From the experimental results and numerical computation, it is seen that the slip distribution can be assumed to be linear with good reasons. So the test results can

be applied in the finite element analysis directly. The result of the test is consistent with the calculation result. So we consider the test result is correct and reasonable.

(4) In our test, the specimens of Group 20 and 30 all demonstrated brittle failure. The reason postulated as following:

The first reason is that when the load approaches the peak point, there is a lot of strain energy stored in the specimen. The strain energy will release while the specimen fails. If the specimen is relatively small, the constraint of the load-application-device is relatively large, which limits the speed of the strain energy releasing and the width of the cracks' extending. However, when the specimen is large, the limitation is relatively small. So the strain energy releases very quickly, the fracture cracks extend too wide and the specimen fails brittle. Because Specimen 20-3 has initial internal damage, the ultimate load is much lower than the other's and the strain energy stored in it is much smaller, too. So when it fails, the cracks extend smaller and it can still keep some soften stage.

The second reason is that when the size of the specimen is large, it is difficult to let the constraint force act on the PVC pipe absolutely evenly along the circumference. So if the constraint force is just act on three or four point, it will cause secondary bending moment. When bond-slip cracks appear on the center of top surface, there will be a large stress concentration caused by the secondary bending moment. It will speed the extension of the cracks and the fail will seem to be brittle.

As time is very limited in my final year project (There are only two and a half months from I came to NTU to I turned in my FYP report.), time is not enough to deal with some other work associated to the project. However the experimental test have been finished successfully and some initial test results have been obtained. For further research work in this project, a new bond-slip model could be set up with the test results. I think there will be some meanings of our test to the understanding of reinforcement concrete.

REFERENCES

1. Liu Yu, (1999), “Computational experiment of composite structural element using damage mechanics”, First Year Report, CSE, NTU.

2. Jiang Jianjing, (1995), “Nonlinear Finite Element Analysis of Concrete Structure”, Tsinghua University Press.

3. Kang Qingliang, (1996), “Finite Element Analysis of RC”, China Hydraulic Power Press

4. Jiang Jianjing, (1998), “Concrete Structure Engineering”, China Building Industry Press.

5. Teng Zhiming, (1985), “Reinforced-concrete Structure”, China Building Industry Press.

6. Jing Zhisheng, (1985), “Experimental Study on the Bond between Steel Bar and Concrete”, J. Southeast University (China), Vol. 2, 1985

7. Song Yupu, (1987), “Experimental Study on the Bond-slip Character between Steel Bar and Concrete”, J. Dalian Technological University (China), Vol. 2, 1987.

8. Teng Zhiming, (1992), “The Inclined Compression Bond Model in the FEA of RC”, J. Engineering Mechanics (China), Vol. 1, 1995.

9. “MARC PRIMER”, (1998), MARC Analysis Research Corporation.

10. “Manual of Sap 91”, (1996), Tsinghua University Press.

11. “”Manual of Sikadur 31”, Sika Pte. Ltd.